



Guided quantum dynamics

Pavel Exner

Doppler Institute

*for Mathematical Physics and Applied Mathematics
Prague*

With thanks to all my collaborators

A minicourse at the **SOMPATY Summer School**
on Mathematics for the Micro/Nano-World

Samarkand, September 11-16, 2023

Quantum waveguides



We return to graphs later, now let us change the topic. Using graphs to model real-world objects like semiconductor *quantum wires* we make certainly some idealizations:

Quantum waveguides



We return to graphs later, now let us change the topic. Using graphs to model real-world objects like semiconductor *quantum wires* we make certainly some idealizations:

- real wires have a *nonzero diameter*

Quantum waveguides



We return to graphs later, now let us change the topic. Using graphs to model real-world objects like semiconductor *quantum wires* we make certainly some idealizations:

- real wires have a *nonzero diameter*
- the confinement is not perfect, in particular, quantum *tunneling* is possible between different wires (or different part of the same wire)

Let us deal with the first point, forgetting temporarily about the possibility of tunneling

Quantum waveguides



We return to graphs later, now let us change the topic. Using graphs to model real-world objects like semiconductor *quantum wires* we make certainly some idealizations:

- real wires have a *nonzero diameter*
- the confinement is not perfect, in particular, quantum *tunneling* is possible between different wires (or different part of the same wire)

Let us deal with the first point, forgetting temporarily about the possibility of tunneling; suppose for starters that we are in a 2D situation and the particle is confined to a *strip of width $2a$* in the plane with *hard walls*.

Quantum waveguides



We return to graphs later, now let us change the topic. Using graphs to model real-world objects like semiconductor *quantum wires* we make certainly some idealizations:

- real wires have a *nonzero diameter*
- the confinement is not perfect, in particular, quantum *tunneling* is possible between different wires (or different part of the same wire)

Let us deal with the first point, forgetting temporarily about the possibility of tunneling; suppose for starters that we are in a 2D situation and the particle is confined to a *strip of width $2a$* in the plane with *hard walls*.

In the absence of other forces, the Hamiltonian is then the (negative) *Laplacian*, $-\Delta$, and the spectral problem means to solve the equation

$$-\left(\frac{\partial^2}{\partial x^2} + \frac{\partial^2}{\partial y^2}\right)\psi(x, y) = \lambda\psi(x, y), \quad x \in \mathbb{R}, |y| < a,$$

with *Dirichlet boundary condition* describing the hard wall, that is

$$\psi(x, \pm a) = 0.$$

A 2D quantum waveguide

This is easy to solve by *separation of variables*



A 2D quantum waveguide



This is easy to solve by *separation of variables*: the transverse problem, $-\chi''(y) = \kappa^2 \chi(y)$, has a discrete spectrum,

$$\kappa_n^2 = \left(\frac{\pi n}{2a}\right)^2, \quad \chi_{2n-1}(y) = \frac{1}{\sqrt{a}} \cos \kappa_{2n-1} y, \quad \chi_{2n}(y) = \frac{1}{\sqrt{a}} \sin \kappa_{2n} y, \quad n = 1, 2, \dots,$$

A 2D quantum waveguide



This is easy to solve by *separation of variables*: the transverse problem, $-\chi''(y) = \kappa^2 \chi(y)$, has a discrete spectrum,

$$\kappa_n^2 = \left(\frac{\pi n}{2a}\right)^2, \quad \chi_{2n-1}(y) = \frac{1}{\sqrt{a}} \cos \kappa_{2n-1} y, \quad \chi_{2n}(y) = \frac{1}{\sqrt{a}} \sin \kappa_{2n} y, \quad n = 1, 2, \dots,$$

while the spectrum of the longitudinal part is $[0, \infty)$

A 2D quantum waveguide



This is easy to solve by *separation of variables*: the transverse problem, $-\chi''(y) = \kappa^2 \chi(y)$, has a discrete spectrum,

$$\kappa_n^2 = \left(\frac{\pi n}{2a}\right)^2, \quad \chi_{2n-1}(y) = \frac{1}{\sqrt{a}} \cos \kappa_{2n-1} y, \quad \chi_{2n}(y) = \frac{1}{\sqrt{a}} \sin \kappa_{2n} y, \quad n = 1, 2, \dots,$$

while the spectrum of the longitudinal part is $[0, \infty)$. Consequently, the spectrum of the full problem is $[\kappa_1^2, \infty)$ with the *generalized eigenfunctions*

$$\chi_n(y) e^{\pm i k x} \quad \text{referring to energy } \kappa_n^2 + k^2$$

A 2D quantum waveguide



This is easy to solve by *separation of variables*: the transverse problem, $-\chi''(y) = \kappa^2 \chi(y)$, has a discrete spectrum,

$$\kappa_n^2 = \left(\frac{\pi n}{2a}\right)^2, \quad \chi_{2n-1}(y) = \frac{1}{\sqrt{a}} \cos \kappa_{2n-1} y, \quad \chi_{2n}(y) = \frac{1}{\sqrt{a}} \sin \kappa_{2n} y, \quad n = 1, 2, \dots,$$

while the spectrum of the longitudinal part is $[0, \infty)$. Consequently, the spectrum of the full problem is $[\kappa_1^2, \infty)$ with the *generalized eigenfunctions*

$$\chi_n(y) e^{\pm ikx} \quad \text{referring to energy } \kappa_n^2 + k^2$$

It is so simple that you may wonder why I am mentioning it at all. The reason will become obvious when we note a *nontrivial geometry* may change the picture. As the simplest example suppose that the *strip is bent*.

A 2D quantum waveguide



This is easy to solve by *separation of variables*: the transverse problem, $-\chi''(y) = \kappa^2 \chi(y)$, has a discrete spectrum,

$$\kappa_n^2 = \left(\frac{\pi n}{2a}\right)^2, \quad \chi_{2n-1}(y) = \frac{1}{\sqrt{a}} \cos \kappa_{2n-1} y, \quad \chi_{2n}(y) = \frac{1}{\sqrt{a}} \sin \kappa_{2n} y, \quad n = 1, 2, \dots,$$

while the spectrum of the longitudinal part is $[0, \infty)$. Consequently, the spectrum of the full problem is $[\kappa_1^2, \infty)$ with the *generalized eigenfunctions*

$$\chi_n(y) e^{\pm i k x} \quad \text{referring to energy } \kappa_n^2 + k^2$$

It is so simple that you may wonder why I am mentioning it at all. The reason will become obvious when we note a *nontrivial geometry* may change the picture. As the simplest example suppose that the *strip is bent*.

To be specific, consider a curve $\Gamma : \mathbb{R} \rightarrow \mathbb{R}^2$ assuming that it is *smooth* and *asymptotically straight* and put $\Omega := \{x \in \mathbb{R}^2 : \text{dist}(x, \Gamma) < a\}$; the strip considered above, which we denote as Ω_0 , refers naturally to the trivial situation when Γ is a straight line.

A bent Dirichlet strip

Classical intuition suggests that *nothing much happens*: the particle may reflect from the walls but *the only closed trajectories* are those perpendicular to the strip axis, a zero measure set in the phase space.



A bent Dirichlet strip



Classical intuition suggests that *nothing much happens*: the particle may reflect from the walls but *the only closed trajectories* are those perpendicular to the strip axis, a zero measure set in the phase space.

To see what happens with a quantum particle, we have to solve the spectral problem, $-\Delta_D^{\Omega} \psi = \lambda \psi$, for the corresponding Dirichlet Laplacian

A bent Dirichlet strip



Classical intuition suggests that *nothing much happens*: the particle may reflect from the walls but *the only closed trajectories* are those perpendicular to the strip axis, a zero measure set in the phase space.

To see what happens with a quantum particle, we have to solve the spectral problem, $-\Delta_{\mathbb{D}}^{\Omega} \psi = \lambda \psi$, for the corresponding Dirichlet Laplacian. A useful trick is to parametrize Ω using locally orthogonal *curvilinear coordinates* s, u , parallel and perpendicular to the strip axis, respectively,

$$x(s, u) = (\Gamma_1(s) - u\dot{\Gamma}_2(s), \Gamma_2(s) + u\dot{\Gamma}_1(s)), \quad |u| < a.$$

A bent Dirichlet strip



Classical intuition suggests that *nothing much happens*: the particle may reflect from the walls but *the only closed trajectories* are those perpendicular to the strip axis, a zero measure set in the phase space.

To see what happens with a quantum particle, we have to solve the spectral problem, $-\Delta_{\mathbb{D}}\psi = \lambda\psi$, for the corresponding Dirichlet Laplacian. A useful trick is to parametrize Ω using locally orthogonal *curvilinear coordinates* s, u , parallel and perpendicular to the strip axis, respectively,

$$x(s, u) = (\Gamma_1(s) - u\dot{\Gamma}_2(s), \Gamma_2(s) + u\dot{\Gamma}_1(s)), \quad |u| < a.$$

We transform $-\Delta$ into these coordinates and remove the Jacobian replacing, with an abuse of notation, $\psi(x)$ with $(1 + u\gamma(s))^{1/2}\psi(s, u)$, where $\gamma(s) := (\ddot{\Gamma}_2\dot{\Gamma}_1 - \ddot{\Gamma}_1\dot{\Gamma}_2)(s)$ is the *signed curvature* of Γ ; then we have to find the spectrum of the following Dirichlet operator in $L^2(\Omega_0)$:

$$H = -\frac{\partial}{\partial s}(1 + u\gamma(s))^{-2}\frac{\partial}{\partial s} - \frac{\partial^2}{\partial u^2} + V(s, u),$$
$$V(s, u) := -\frac{\gamma(s)^2}{4(1 + u\gamma(s))^2} + \frac{u\ddot{\gamma}(s)}{2(1 + u\gamma(s))^3} - \frac{5}{4}\frac{u^2\dot{\gamma}(s)^2}{(1 + u\gamma(s))^4}.$$

A bent Dirichlet strip



In this way, we have to solve an equation on a straight strip but a more complicated; the geometry was now *translated into the coefficients*.

A bent Dirichlet strip



In this way, we have to solve an equation on a straight strip but a more complicated; the geometry was now *translated into the coefficients*.

It is not as bad as it looks at a glance. First of all, since Ω is supposed to be *asymptotically straight*, it is easy to check that the bend keeps the essential spectrum preserved, $\sigma_{\text{ess}}(-\Delta_D^\Omega) = [\kappa_1^2, \infty)$

A bent Dirichlet strip



In this way, we have to solve an equation on a straight strip but a more complicated; the geometry was now *translated into the coefficients*.

It is not as bad as it looks at a glance. First of all, since Ω is supposed to be *asymptotically straight*, it is easy to check that the bend keeps the essential spectrum preserved, $\sigma_{\text{ess}}(-\Delta_D^\Omega) = [\kappa_1^2, \infty)$. Moreover, we have

$$H = -\frac{\partial^2}{\partial u^2} - \frac{\partial^2}{\partial s^2} - \frac{1}{4}\gamma(s)^2 + \mathcal{O}(a) \quad \text{as } a \rightarrow 0,$$

and as a 1D Schrödinger operator with a *purely attractive potential*, the longitudinal part has *at least one negative eigenvalues* whenever $\gamma \neq 0$.

A bent Dirichlet strip



In this way, we have to solve an equation on a straight strip but a more complicated; the geometry was now *translated into the coefficients*.

It is not as bad as it looks at a glance. First of all, since Ω is supposed to be *asymptotically straight*, it is easy to check that the bend keeps the essential spectrum preserved, $\sigma_{\text{ess}}(-\Delta_D^\Omega) = [\kappa_1^2, \infty)$. Moreover, we have

$$H = -\frac{\partial^2}{\partial u^2} - \frac{\partial^2}{\partial s^2} - \frac{1}{4}\gamma(s)^2 + \mathcal{O}(a) \quad \text{as } a \rightarrow 0,$$

and as a 1D Schrödinger operator with a *purely attractive potential*, the longitudinal part has *at least one negative eigenvalues* whenever $\gamma \neq 0$.

Remark: Limits like $a \rightarrow 0$ were studied in the 1970s as a tool for *quantization on manifolds*. In particular, Jiří Tolar computed them in all dimensions and codimensions

A bent Dirichlet strip



In this way, we have to solve an equation on a straight strip but a more complicated; the geometry was now *translated into the coefficients*.

It is not as bad as it looks at a glance. First of all, since Ω is supposed to be *asymptotically straight*, it is easy to check that the bend keeps the essential spectrum preserved, $\sigma_{\text{ess}}(-\Delta_D^\Omega) = [\kappa_1^2, \infty)$. Moreover, we have

$$H = -\frac{\partial^2}{\partial u^2} - \frac{\partial^2}{\partial s^2} - \frac{1}{4}\gamma(s)^2 + \mathcal{O}(a) \quad \text{as } a \rightarrow 0,$$

and as a 1D Schrödinger operator with a *purely attractive potential*, the longitudinal part has *at least one negative eigenvalues* whenever $\gamma \neq 0$.

Remark: Limits like $a \rightarrow 0$ were studied in the 1970s as a tool for *quantization on manifolds*. In particular, Jiří Tolar computed them in all dimensions and codimensions – but his supervisor told him it was good for nothing so he put it into his drawer and published it only many years later:



J. Tolar: On a quantum mechanical d'Alembert principle, in *Group Theoretical Methods in Physics*, Lecture Notes in Physics, vol. 313, Springer, Berlin 1988; pp. 268-274.

A bent Dirichlet strip



In this way, we have to solve an equation on a straight strip but a more complicated; the geometry was now *translated into the coefficients*.

It is not as bad as it looks at a glance. First of all, since Ω is supposed to be *asymptotically straight*, it is easy to check that the bend keeps the essential spectrum preserved, $\sigma_{\text{ess}}(-\Delta_D^\Omega) = [\kappa_1^2, \infty)$. Moreover, we have

$$H = -\frac{\partial^2}{\partial u^2} - \frac{\partial^2}{\partial s^2} - \frac{1}{4}\gamma(s)^2 + \mathcal{O}(a) \quad \text{as } a \rightarrow 0,$$

and as a 1D Schrödinger operator with a *purely attractive potential*, the longitudinal part has *at least one negative eigenvalues* whenever $\gamma \neq 0$.

Remark: Limits like $a \rightarrow 0$ were studied in the 1970s as a tool for *quantization on manifolds*. In particular, Jiří Tolar computed them in all dimensions and codimensions – but his supervisor told him it was good for nothing so he put it into his drawer and published it only many years later:



J. Tolar: On a quantum mechanical d'Alembert principle, in *Group Theoretical Methods in Physics*, Lecture Notes in Physics, vol. 313, Springer, Berlin 1988; pp. 268-274.

Moral: Listen to your supervisor, but think twice before taking his advice!

A bent Dirichlet strip



But we can do better, without restriction on the strip width. Consider any $a > 0$ for which the strip boundary is still smooth, $a\|\gamma\|_\infty < 1$, and the strip *does not intersect itself*.

A bent Dirichlet strip



But we can do better, without restriction on the strip width. Consider any $a > 0$ for which the strip boundary is still smooth, $a\|\gamma\|_\infty < 1$, and the strip *does not intersect itself*.

We apply the *variational method*: if we find a function $\phi \in D(H)$ such that $(\psi, H\psi) < \kappa_1^2 \|\psi\|^2$, the spectrum threshold would be *below* κ_1^2 .

A bent Dirichlet strip



But we can do better, without restriction on the strip width. Consider any $a > 0$ for which the strip boundary is still smooth, $a\|\gamma\|_\infty < 1$, and the strip *does not intersect itself*.

We apply the *variational method*: if we find a function $\phi \in D(H)$ such that $(\psi, H\psi) < \kappa_1^2 \|\psi\|^2$, the spectrum threshold would be *below* κ_1^2 .

Using the Ansatz $\psi(s, u) = \phi_\lambda(s)\chi_1(u) + \varepsilon f(s, u)$, one can check that choosing appropriately functions $\phi_\lambda(s)$ and f and the number ε , we achieve the goal obtaining the following result:

Theorem

If the strip axis is a C^4 smooth curve, not straight but asymptotically straight [leaving out the precise formulation], the Dirichlet Laplacian in the curved strip has at least one isolated eigenvalue below κ_1^2 .



J. Goldstone, R.L. Jaffe: Bound states in twisting tubes, *Phys. Rev.* **B45** (1992), 14100–14107.



P. Duclos, P.E.: Curvature-induced bound states in quantum waveguides in two and three dimensions, *Rev. Math. Phys.* **7** (1995), 73–102.

How it differs from the classical motion?



Trying to understand where this effect might come from we may think of what classical mechanics tells us about a *bobsleigh* moving down through a twisting, banked, iced track

How it differs from the classical motion?



Trying to understand where this effect might come from we may think of what classical mechanics tells us about a *bobsleigh* moving down through a twisting, banked, iced track. As we all know in the curved part the conservation laws make the bobsleigh 'climb' the track wall,



Source: Wikipedia

How it differs from the classical motion?



Trying to understand where this effect might come from we may think of what classical mechanics tells us about a *bobsleigh* moving down through a twisting, banked, iced track. As we all know in the curved part the conservation laws make the bobsleigh 'climb' the track wall,



Source: Wikipedia

However, for a 'quantum bobsleigh' the transverse contribution to the energy is *quantized* so it may not be able to 'jump' from one transverse level to another one.

How it differs from the classical motion?



Trying to understand where this effect might come from we may think of what classical mechanics tells us about a *bobsleigh* moving down through a twisting, banked, iced track. As we all know in the curved part the conservation laws make the bobsleigh 'climb' the track wall,



Source: Wikipedia

However, for a 'quantum bobsleigh' the transverse contribution to the energy is *quantized* so it may not be able to 'jump' from one transverse level to another one.

The comparison is only partly fitting, of course, one can note that a bobsleigh in a rectangular-shaped track would climb nowhere.

Smoothness is not obligatory



What is important, the effect of *geometrically induced binding* is *robust*.

Smoothness is not obligatory



What is important, the effect of *geometrically induced binding* is *robust*.

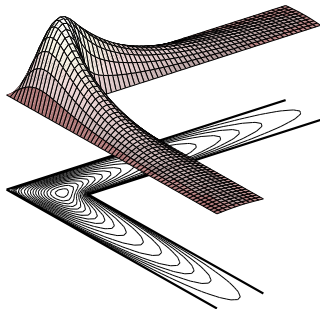
To illustrate this claim, consider Ω in the shape of an *L-shaped strip*; we choose the width $2a = \pi$ so that $\kappa_1^2 = 1$

Smoothness is not obligatory



What is important, the effect of *geometrically induced binding* is *robust*.

To illustrate this claim, consider Ω in the shape of an *L-shaped strip*; we choose the width $2a = \pi$ so that $\kappa_1^2 = 1$. Expanding the sought solution to $-\Delta_{\mathbb{D}}^{\Omega} \psi = \lambda \psi$ into the 'transverse' basis, one can prove that the operator has a single eigenvalue ≈ 0.929 ; the corresponding eigenfunction is



P.E., P. Šeba, P. Štoviček: On existence of a bound state in an L-shaped waveguide, *Czech. J. Phys.* **B39** (1989), 1181–1191.

Other geometries



Moreover, the binding effect coming from the geometry of the guide is *not restricted to bends*. For instance, it is not difficult to see that bound states occur if the tube has a local *'bulge'*.

Other geometries



Moreover, the binding effect coming from the geometry of the guide is *not restricted to bends*. For instance, it is not difficult to see that bound states occur if the tube has a local *'bulge'*.

Similar effect can also be seen in more complicated geometries. Consider, for instance, a pair of *parallel Dirichlet strips* of widths d_1 , d_2 and suppose they are connected laterally by *window of width a* in the common boundary

Other geometries



Moreover, the binding effect coming from the geometry of the guide is *not restricted to bends*. For instance, it is not difficult to see that bound states occur if the tube has a local *'bulge'*.

Similar effect can also be seen in more complicated geometries. Consider, for instance, a pair of *parallel Dirichlet strips* of widths d_1 , d_2 and suppose they are connected laterally by *window of width a* in the common boundary

The *essential* (absolutely continuous) *spectrum* of the Hamiltonian H starts now at $(\frac{\pi}{d})^2$, where $d = \max\{d_1, d_2\}$ and we have

Theorem

The discrete spectrum of H is *nonempty* for any $a > 0$ and

$$\#\sigma_{\text{disc}}(H) \geq \frac{2a}{d} \sqrt{1 - \left(\frac{d}{d_1 + d_2}\right)^2}$$



P.E., P. Šeba, M. Tater, D. Vaněk: Bound states and scattering in quantum waveguides coupled laterally through a boundary window, *J. Math. Phys.* **37** (1996), 4867–4887.

Example: two particular cases

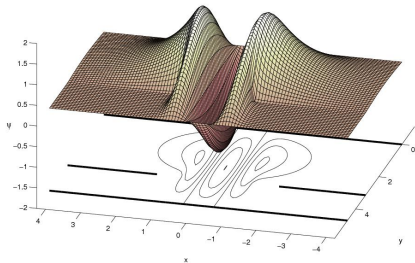
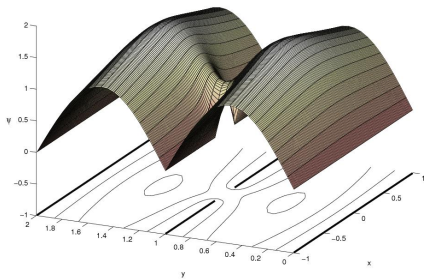


Let us plot two eigenfunction, the *ground state* for $d_1 = d_2$ and the *second excited state* is an asymmetric waveguide:

Example: two particular cases



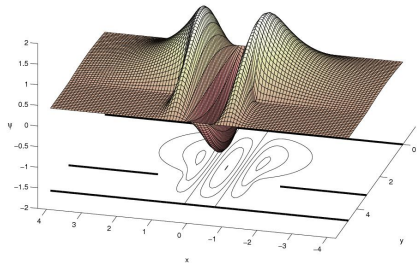
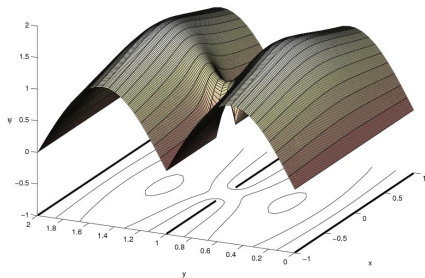
Let us plot two eigenfunction, the *ground state* for $d_1 = d_2$ and the *second excited state* is an asymmetric waveguide:



Example: two particular cases



Let us plot two eigenfunction, the *ground state* for $d_1 = d_2$ and the *second excited state* is an asymmetric waveguide:

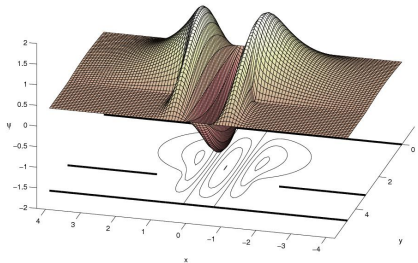
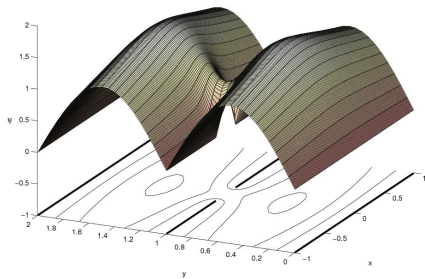


In particular, this example illustrates well the *purely quantum nature* of the effect

Example: two particular cases



Let us plot two eigenfunction, the *ground state* for $d_1 = d_2$ and the *second excited state* is an asymmetric waveguide:



In particular, this example illustrates well the *purely quantum nature* of the effect: a classical particle in such a system *cannot be trapped* except for the (*phase-space measure zero!*) events of reflections, either from the window edges or perpendicular to the walls.

A detour: Šeba billiard



Of course, this is not the only example illustrating *profound differences* between the classical and quantum mechanics. Let us mention one more, remotely related, which concerns a *chaotic behavior*.

A detour: Šeba billiard



Of course, this is not the only example illustrating *profound differences* between the classical and quantum mechanics. Let us mention one more, remotely related, which concerns a *chaotic behavior*.

In the canonical chaotic behavior example of *Sinai billiard*, shrinking the obstacle to a point, the system becomes *integrable*.

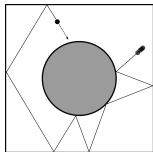
A detour: Šeba billiard



Of course, this is not the only example illustrating *profound differences* between the classical and quantum mechanics. Let us mention one more, remotely related, which concerns a *chaotic behavior*.

In the canonical chaotic behavior example of *Sinai billiard*, shrinking the obstacle to a point, the system becomes *integrable*.

Quantum chaos shows in the *eigenvalue spacing distribution*, and the quantum Sinai billiard *remains chaotic* even if the obstacle is a *point interaction* – although *not fully chaotic* in the sense of GOE ensemble. What is important, such an effect was also *observed experimentally*.



Source: wikipedia

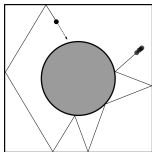
A detour: Šeba billiard



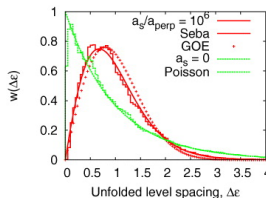
Of course, this is not the only example illustrating *profound differences* between the classical and quantum mechanics. Let us mention one more, remotely related, which concerns a *chaotic behavior*.

In the canonical chaotic behavior example of *Sinai billiard*, shrinking the obstacle to a point, the system becomes *integrable*.

Quantum chaos shows in the *eigenvalue spacing distribution*, and the quantum Sinai billiard *remains chaotic* even if the obstacle is a *point interaction* – although *not fully chaotic* in the sense of GOE ensemble. What is important, such an effect was also *observed experimentally*.



Source: wikipedia



Source: [SAYO'10]



P. Šeba: Wave chaos in singular quantum billiard, *Phys. Rev. Lett.* **64** (1990), 1855–1858.



C. Stone, Y.A. El Aoudi, V.A. Yurovsky, M. Olshani1: Two simple systems with cold atoms: quantum chaos tests and non-equilibrium dynamics, *New J. Phys.* **12** (2010), 055022.

More results about waveguides



- The results can be tested experimentally in *flat electromagnetic waveguides*.



J.T. Londergan, J.P. Carini, D.P. Murdock: *Binding and Scattering in Two-Dimensional Systems. Applications to Quantum Wires, Waveguides and Photonic Crystals*, Springer LNP m60, Berlin 1999.

More results about waveguides



- The results can be tested experimentally in *flat electromagnetic waveguides*.



J.T. Londergan, J.P. Carini, D.P. Murdock: *Binding and Scattering in Two-Dimensional Systems. Applications to Quantum Wires, Waveguides and Photonic Crystals*, Springer LNP m60, Berlin 1999.

- Similar results hold for other boundary conditions *except Neumann*

More results about waveguides



- The results can be tested experimentally in *flat electromagnetic waveguides*.



J.T. Londergan, J.P. Carini, D.P. Murdock: *Binding and Scattering in Two-Dimensional Systems. Applications to Quantum Wires, Waveguides and Photonic Crystals*, Springer LNP m60, Berlin 1999.

- Similar results hold for other boundary conditions *except Neumann*. However, if the boundaries are different, the orientation matters, e.g., in a DN strip a bending produces bound states if the Dirichlet condition is *'inside'* and it *does not* in the opposite case.



J. Dittrich, J. Kříž: Curved planar quantum wires with Dirichlet and Neumann boundary conditions, *J. Phys. A: Math. Gen.* **35** (2002), L269–275.

More results about waveguides



- The results can be tested experimentally in *flat electromagnetic waveguides*.



J.T. Londergan, J.P. Carini, D.P. Murdock: *Binding and Scattering in Two-Dimensional Systems. Applications to Quantum Wires, Waveguides and Photonic Crystals*, Springer LNP m60, Berlin 1999.

- Similar results hold for other boundary conditions *except Neumann*. However, if the boundaries are different, the orientation matters, e.g., in a DN strip a bending produces bound states if the Dirichlet condition is *'inside'* and it *does not* in the opposite case.



J. Dittrich, J. Kříž: Curved planar quantum wires with Dirichlet and Neumann boundary conditions, *J. Phys. A: Math. Gen.* **35** (2002), L269–275.

- Similar results hold for three-dimensional bent tubes of *circular cross section*.

More results about waveguides



- The results can be tested experimentally in *flat electromagnetic waveguides*.



J.T. Londergan, J.P. Carini, D.P. Murdock: *Binding and Scattering in Two-Dimensional Systems. Applications to Quantum Wires, Waveguides and Photonic Crystals*, Springer LNP m60, Berlin 1999.

- Similar results hold for other boundary conditions *except Neumann*. However, if the boundaries are different, the orientation matters, e.g., in a DN strip a bending produces bound states if the Dirichlet condition is *'inside'* and it *does not* in the opposite case.



J. Dittrich, J. Kříž: Curved planar quantum wires with Dirichlet and Neumann boundary conditions, *J. Phys. A: Math. Gen.* **35** (2002), L269–275.

- Similar results hold for three-dimensional bent tubes of *circular cross section*.
- If the cross section *is not circular*, we have to consider the *twisting* which, in contrast to the bending, produces a *repulsive* interaction.

For many more results see



P.E., H. Kovařík: *Quantum Waveguides*; xxii + 382 p.; Springer International, Heidelberg 2015.

Quantum layers



If we take this exercise *one dimension higher*, we can observe other interesting phenomena

Quantum layers

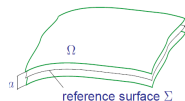


If we take this exercise *one dimension higher*, we can observe other interesting phenomena. Such situations have again a physical meaning, say, as models of electrons in semiconductor *layers on a non-flat substrate*.

Quantum layers



If we take this exercise *one dimension higher*, we can observe other interesting phenomena. Such situations have again a physical meaning, say, as models of electrons in semiconductor *layers on a non-flat substrate*.

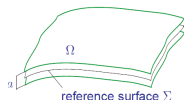


We consider a particle confined to a *hard-wall layer* of width $2a$ built over an *infinite, smooth, non-planar, asymptotically flat* surface Σ

Quantum layers



If we take this exercise *one dimension higher*, we can observe other interesting phenomena. Such situations have again a physical meaning, say, as models of electrons in semiconductor *layers on a non-flat substrate*.



We consider a particle confined to a *hard-wall layer* of width $2a$ built over an *infinite, smooth, non-planar, asymptotically flat* surface Σ . As in the previous case we can use the curvilinear coordinates in which, for *thin layers*, we have

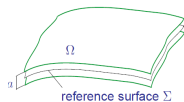
$$H = -\frac{\partial^2}{\partial u^2} - g^{-1/2} \frac{\partial}{\partial s_\mu} g^{1/2} g^{\mu\nu} \frac{\partial}{\partial s_\nu} + K - M^2 + \mathcal{O}(a),$$

where g is *metric tensor* of the surface Σ , and K , M are its *Gauss* and *mean* curvatures, respectively

Quantum layers



If we take this exercise *one dimension higher*, we can observe other interesting phenomena. Such situations have again a physical meaning, say, as models of electrons in semiconductor *layers on a non-flat substrate*.



We consider a particle confined to a *hard-wall layer* of width $2a$ built over an *infinite, smooth, non-planar, asymptotically flat* surface Σ . As in the previous case we can use the curvilinear coordinates in which, for *thin layers*, we have

$$H = -\frac{\partial^2}{\partial u^2} - g^{-1/2} \frac{\partial}{\partial s_\mu} g^{1/2} g^{\mu\nu} \frac{\partial}{\partial s_\nu} + K - M^2 + \mathcal{O}(a),$$

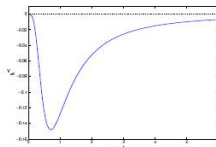
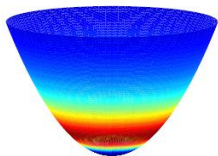
where g is *metric tensor* of the surface Σ , and K , M are its *Gauss* and *mean* curvatures, respectively. Since $K = k_1 k_2$ and $M = \frac{1}{2}(k_1 + k_2)$, the leading term of the effective potential, $K - M^2 = -\frac{1}{4}(k_1 - k_2)^2$, is again of the *attractive* nature, vanishing only on *planes* and *spheres*.

The effective potential in a thin layer

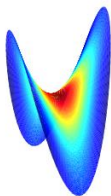


Effective Potential $V_{\text{eff}} = -\frac{1}{4}(k_+ - k_-)^2$

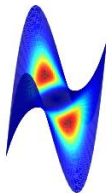
Paraboloid of Revolution $z = x^2 + y^2$



Hyperbolic Paraboloid $z = x^2 - y^2$



Monkey Saddle $z = x^3 - 3xy^2$



The minima of V_{eff} are marked by the dark red colour.

Curvature induced bound states in layers

However, the existence results are not limited to thin layers only:



Curvature induced bound states in layers



However, the existence results are not limited to thin layers only:

Theorem

If the surface Σ is C^4 smooth *non-planar* and $\mathcal{K} = \int_{\Sigma} K \, d\Sigma \leq 0$ we have $\inf \sigma(H) < \kappa_1^2$. If Σ is *asymptotically flat* [leaving out again the precise formulation], the the Dirichlet Laplacian has *at least one isolated eigenvalue* below κ_1^2 .



P. Duclos, P.E., H. Krejčířík: Bound states in curved quantum layers, *Commun. Math. Phys.* **223** (2001), 13–28.

Curvature induced bound states in layers



However, the existence results are not limited to thin layers only:

Theorem

If the surface Σ is C^4 smooth *non-planar* and $\mathcal{K} = \int_{\Sigma} K d\Sigma \leq 0$ we have $\inf \sigma(H) < \kappa_1^2$. If Σ is *asymptotically flat* [leaving out again the precise formulation], the the Dirichlet Laplacian has *at least one isolated eigenvalue* below κ_1^2 .

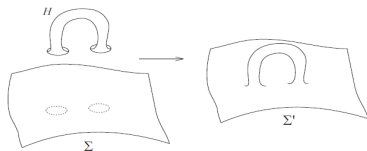


P. Duclos, P.E., H. Krejčířik: Bound states in curved quantum layers, *Commun. Math. Phys.* **223** (2001), 13–28.

Furthermore, the *Cohn-Vossen inequality* states that

$$\mathcal{K} \leq 2\pi(2 - 2h - e),$$

where h is the *genus* of Σ and e is the *number of ends*



Nontrivial topology & positive Gauss curvature



Hence $\mathcal{K} < 0$ whenever $h \geq 1$ and we have

Theorem

*Conclusions of the previous theorem hold whenever Σ is **not** conformally equivalent to the plane.*



G. Carron, P.E., D. Krejčířík: Topologically non-trivial quantum layers, *J. Math. Phys.* **45** (2004), 774–784.

Nontrivial topology & positive Gauss curvature



Hence $\mathcal{K} < 0$ whenever $h \geq 1$ and we have

Theorem

*Conclusions of the previous theorem hold whenever Σ is **not** conformally equivalent to the plane.*



G. Carron, P.E., D. Krejčířík: Topologically non-trivial quantum layers, *J. Math. Phys.* **45** (2004), 774–784.

In the opposite situation, $\mathcal{K} > 0$, we do not have such a universal result, just several *sufficient conditions*

Nontrivial topology & positive Gauss curvature



Hence $\mathcal{K} < 0$ whenever $h \geq 1$ and we have

Theorem

*Conclusions of the previous theorem hold whenever Σ is **not** conformally equivalent to the plane.*



G. Carron, P.E., D. Krejčířík: Topologically non-trivial quantum layers, *J. Math. Phys.* **45** (2004), 774–784.

In the opposite situation, $\mathcal{K} > 0$, we do not have such a universal result, just several *sufficient conditions*. As you may expect, one of them guarantees the existence of curvature induced bound states provided *the layer halfwidth a is small enough*.

Nontrivial topology & positive Gauss curvature



Hence $\mathcal{K} < 0$ whenever $h \geq 1$ and we have

Theorem

*Conclusions of the previous theorem hold whenever Σ is **not** conformally equivalent to the plane.*



G. Carron, P.E., D. Krejčířík: Topologically non-trivial quantum layers, *J. Math. Phys.* **45** (2004), 774–784.

In the opposite situation, $\mathcal{K} > 0$, we do not have such a universal result, just several *sufficient conditions*. As you may expect, one of them guarantees the existence of curvature induced bound states provided *the layer halfwidth a is small enough*.

But layers of positive Gauss curvature reveal other interesting property, namely that the spectral properties may depend on the *global geometry* of the region to which the particle is confined.

Example: conical layers



Consider a hard-wall layer of the thickness π built over *conical surface* of an opening angle $\pi - 2\theta$ for some $\theta \in (0, \frac{1}{2}\pi)$,

$$\Sigma_\theta := \{(r, \phi, z) \in \mathbb{R}^3 : z = r \sin \theta, \phi \in [0, 2\pi)\}$$

Call the corresponding Dirichlet Laplacian H_θ . We have

Example: conical layers



Consider a hard-wall layer of the thickness π built over *conical surface* of an opening angle $\pi - 2\theta$ for some $\theta \in (0, \frac{1}{2}\pi)$,

$$\Sigma_\theta := \{(r, \phi, z) \in \mathbb{R}^3 : z = r \sin \theta, \phi \in [0, 2\pi)\}$$

Call the corresponding Dirichlet Laplacian H_θ . We have

Theorem

For any fixed $\theta \in (0, \frac{1}{2}\pi)$ we have $\sigma_{\text{ess}}(H_\theta) = [1, \infty)$ while the discrete spectrum of the operator is non-empty with $\#\sigma_{\text{disc}}(H_\theta) = \infty$. Each eigenfunction is *axially symmetric*, i.e. independent of ϕ .



P.E., M. Tater: Spectrum of Dirichlet Laplacian in a conical layer, *J. Phys. A: Math. Theor.* **43** (2010), 474023.

Example: conical layers



Consider a hard-wall layer of the thickness π built over *conical surface* of an opening angle $\pi - 2\theta$ for some $\theta \in (0, \frac{1}{2}\pi)$,

$$\Sigma_\theta := \{(r, \phi, z) \in \mathbb{R}^3 : z = r \sin \theta, \phi \in [0, 2\pi)\}$$

Call the corresponding Dirichlet Laplacian H_θ . We have

Theorem

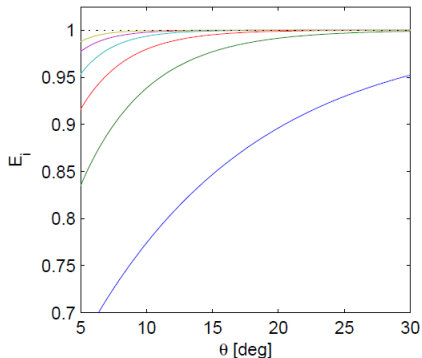
For any fixed $\theta \in (0, \frac{1}{2}\pi)$ we have $\sigma_{\text{ess}}(H_\theta) = [1, \infty)$ while the discrete spectrum of the operator is non-empty with $\#\sigma_{\text{disc}}(H_\theta) = \infty$. Each eigenfunction is *axially symmetric*, i.e. independent of ϕ .



P.E., M. Tater: Spectrum of Dirichlet Laplacian in a conical layer, *J. Phys. A: Math. Theor.* **43** (2010), 474023.

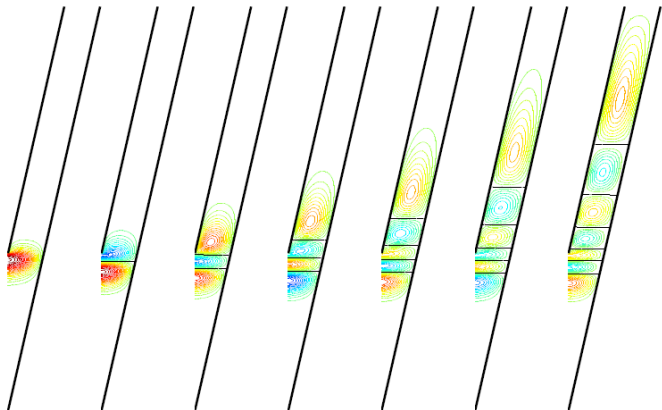
The discrete spectrum infiniteness is related to the fact that the *geodetic circles* on Σ_θ are *shorter* than their counterparts in the plane, which means that the effective attractive potential that behaves asymptotically as $\frac{c}{r^2}$.

Conical layer eigenvalues



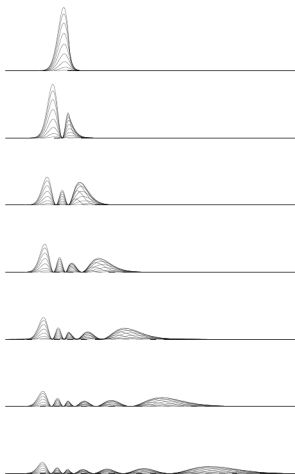
Plot of the dependence of the first six eigenvalues on θ

Conical layer eigenfunctions



Plot of the first seven eigenvalues for $\theta = \frac{5\pi}{36}$

Conical layer probability distributions



Plot of the radial cuts of the first seven probability distributions for $\theta = \frac{5\pi}{36}$

General parabolic layers

In fact, the conical layer represents the *borderline situation* as far as the infiniteness of the discrete spectrum is concerned.



General parabolic layers



In fact, the conical layer represents the *borderline situation* as far as the infiniteness of the discrete spectrum is concerned.

Consider surface of revolution $\Sigma(f) := \{(x, f(|x|)) \in \mathbb{R}^3 : x \in \mathbb{R}^2\}$ corresponding to a function $f \in C^\infty$ such that $f(0) = \dot{f}(0) = 0$ and $f(r) = cr^\alpha$, $\alpha > 1$, holds for all $r \geq R$

General parabolic layers



In fact, the conical layer represents the *borderline situation* as far as the infiniteness of the discrete spectrum is concerned.

Consider surface of revolution $\Sigma(f) := \{(x, f(|x|)) \in \mathbb{R}^3 : x \in \mathbb{R}^2\}$ corresponding to a function $f \in C^\infty$ such that $f(0) = \dot{f}(0) = 0$ and $f(r) = cr^\alpha$, $\alpha > 1$, holds for all $r \geq R$, and the layer $\Omega = \Omega(f, a)$ of halfwidth a small enough to make the parallel coordinates well defined.

General parabolic layers



In fact, the conical layer represents the *borderline situation* as far as the infiniteness of the discrete spectrum is concerned.

Consider surface of revolution $\Sigma(f) := \{(x, f(|x|)) \in \mathbb{R}^3 : x \in \mathbb{R}^2\}$ corresponding to a function $f \in C^\infty$ such that $f(0) = \dot{f}(0) = 0$ and $f(r) = cr^\alpha$, $\alpha > 1$, holds for all $r \geq R$, and the layer $\Omega = \Omega(f, a)$ of halfwidth a small enough to make the parallel coordinates well defined.

Theorem

We have $\sigma_{\text{ess}}(H) = [(\frac{\pi}{2a})^2, \infty)$ and $\#\sigma_{\text{disc}}(H) = \infty$. Moreover, we have

$$N_{(\frac{\pi}{2a})^2 - E}(H) \approx \frac{1}{2\pi} \frac{\alpha c}{2^\alpha} \frac{B(\frac{3}{2}, \frac{\alpha}{2} - \frac{1}{2})}{E^{(\alpha-1)/2}} \quad \text{as } E \searrow 0,$$

where $B(\cdot, \cdot)$ is the Euler beta function, and $f \approx g$ means $f(z), g(z) \rightarrow \infty$ and $\frac{f(z)}{g(z)} \rightarrow 1$ as $z \rightarrow 0$.



P.E., V. Lotoreichik: Spectral asymptotics of the Dirichlet Laplacian on a generalized parabolic layer, *Int. Eqs Oper. Theory.* **92** (2020), 15

Spiral waveguides



Returning to waveguides, note that not every bending gives rise to a non-void discrete spectrum. To show that, consider *spiral-shaped regions*.

Spiral waveguides



Returning to waveguides, note that not every bending gives rise to a non-void discrete spectrum. To show that, consider *spiral-shaped regions*.

Such waveguide-type systems appear often in physics. A few examples:

- guides for cold atoms with application to atomic gyroscopes



Jiang Xiao-Jun, Li Xiao-Lin, Xu Xin-Ping, Zhang Hai-Chao, Wang Yu-Zhu: Archimedean-spiral-based microchip ring waveguide for cold atoms, *Chinese Phys. Lett.* **32** (2015), 020301.



Xiaojun Jiang, Xiaolin Li, Haichao Zhang, Yuzhu Wang: Smooth Archimedean-spiral ring waveguide for cold atomic gyroscope, *Chinese Opt. Lett.* **14** (2016), 070201.

Spiral waveguides



Returning to waveguides, note that not every bending gives rise to a non-void discrete spectrum. To show that, consider *spiral-shaped regions*.

Such waveguide-type systems appear often in physics. A few examples:

- guides for cold atoms with application to atomic gyroscopes



Jiang Xiao-Jun, Li Xiao-Lin, Xu Xin-Ping, Zhang Hai-Chao, Wang Yu-Zhu: Archimedean-spiral-based microchip ring waveguide for cold atoms, *Chinese Phys. Lett.* **32** (2015), 020301.



Xiaojun Jiang, Xiaolin Li, Haichao Zhang, Yuzhu Wang: Smooth Archimedean-spiral ring waveguide for cold atomic gyroscope, *Chinese Opt. Lett.* **14** (2016), 070201.

- electromagnetic or optical systems



N. Bamiedakis, J. Beals, R.V. Penty, I.H. White, J.V. DeGroot, T.V. Clapp: Cost-effective multimode polymer waveguides for high-speed on-board optical interconnects, *IEEE J. Quant. Electronics* **45** (2009), 415–424.



Zhitian Chen *et al.*: Spiral Bragg grating waveguides for TM mode Silicon photonics, *Optics Express* **23** (2015), 25295–25307.

Spiral waveguides



Returning to waveguides, note that not every bending gives rise to a non-void discrete spectrum. To show that, consider *spiral-shaped regions*.

Such waveguide-type systems appear often in physics. A few examples:

- guides for cold atoms with application to atomic gyroscopes



Jiang Xiao-Jun, Li Xiao-Lin, Xu Xin-Ping, Zhang Hai-Chao, Wang Yu-Zhu: Archimedean-spiral-based microchip ring waveguide for cold atoms, *Chinese Phys. Lett.* **32** (2015), 020301.



Xiaojun Jiang, Xiaolin Li, Haichao Zhang, Yuzhu Wang: Smooth Archimedean-spiral ring waveguide for cold atomic gyroscope, *Chinese Opt. Lett.* **14** (2016), 070201.

- electromagnetic or optical systems



N. Bamiedakis, J. Beals, R.V. Penty, I.H. White, J.V. DeGroot, T.V. Clapp: Cost-effective multimode polymer waveguides for high-speed on-board optical interconnects, *IEEE J. Quant. Electronics* **45** (2009), 415–424.



Zhitian Chen *et al.*: Spiral Bragg grating waveguides for TM mode Silicon photonics, *Optics Express* **23** (2015), 25295–25307.

- with applications such as nanoparticle detection or spectrometry



Shui-Jing Tang *et al.*: On-chip spiral waveguides for ultrasensitive and rapid detection of nanoscale objects, *Advanced Materials* **30** (2018), 1800262.



B. Redding, Seng Fatt Liew, Y. Bromberg, Raktim Sarma, Hui Cao: Evanescently coupled multimode spiral spectrometer, *Optica* **3** (2016), 956–962.



Tong Chen, Hansuek Lee, K.J. Vahala: Design and characterization of whispering-gallery spiral waveguides, *Optics Express* **22** (2014), 5196–5208.

Spiral waveguides



Returning to waveguides, note that not every bending gives rise to a non-void discrete spectrum. To show that, consider *spiral-shaped regions*.

Such waveguide-type systems appear often in physics. A few examples:

- guides for cold atoms with application to atomic gyroscopes



Jiang Xiao-Jun, Li Xiao-Lin, Xu Xin-Ping, Zhang Hai-Chao, Wang Yu-Zhu: Archimedean-spiral-based microchip ring waveguide for cold atoms, *Chinese Phys. Lett.* **32** (2015), 020301.



Xiaojun Jiang, Xiaolin Li, Haichao Zhang, Yuzhu Wang: Smooth Archimedean-spiral ring waveguide for cold atomic gyroscope, *Chinese Opt. Lett.* **14** (2016), 070201.

- electromagnetic or optical systems



N. Bamiedakis, J. Beals, R.V. Penty, I.H. White, J.V. DeGroot, T.V. Clapp: Cost-effective multimode polymer waveguides for high-speed on-board optical interconnects, *IEEE J. Quant. Electronics* **45** (2009), 415–424.



Zhitian Chen *et al.*: Spiral Bragg grating waveguides for TM mode Silicon photonics, *Optics Express* **23** (2015), 25295–25307.

- with applications such as nanoparticle detection or spectrometry



Shui-Jing Tang *et al.*: On-chip spiral waveguides for ultrasensitive and rapid detection of nanoscale objects, *Advanced Materials* **30** (2018), 1800262.



B. Redding, Seng Fatt Liew, Y. Bromberg, Raktim Sarma, Hui Cao: Evanescently coupled multimode spiral spectrometer, *Optica* **3** (2016), 956–962.



Tong Chen, Hansuek Lee, K.J. Vahala: Design and characterization of whispering-gallery spiral waveguides, *Optics Express* **22** (2014), 5196–5208.

- spiral shapes appear also in acoustic waveguides



S. Periyannan, P. Rajagopal, K. Balasubramaniam: Multiple temperature sensors embedded in an ultrasonic “spiral-like” waveguide, *AIP Advances* **7** (2017), 035201.

The simplest case: an Archimedean waveguide



Let Γ_a be the Archimedean spiral in the plane with the slope $a > 0$, expressed in terms of the polar coordinates, $\Gamma_a = \{r = a\theta : \theta \geq 0\}$, and denote by \mathcal{C}_a its complement, $\mathcal{C}_a := \mathbb{R}^2 \setminus \Gamma_a$ which is an open set.



Source: Wikipedia

The simplest case: an Archimedean waveguide



Let Γ_a be the Archimedean spiral in the plane with the slope $a > 0$, expressed in terms of the polar coordinates, $\Gamma_a = \{r = a\theta : \theta \geq 0\}$, and denote by \mathcal{C}_a its complement, $\mathcal{C}_a := \mathbb{R}^2 \setminus \Gamma_a$ which is an open set.



Source: Wikipedia

We are interested in $H_a = -\Delta_{\mathcal{D}}^{\mathcal{C}_a}$, the Dirichlet Laplacian in $L^2(\mathcal{C}_a)$

The simplest case: an Archimedean waveguide



Let Γ_a be the Archimedean spiral in the plane with the slope $a > 0$, expressed in terms of the polar coordinates, $\Gamma_a = \{r = a\theta : \theta \geq 0\}$, and denote by \mathcal{C}_a its complement, $\mathcal{C}_a := \mathbb{R}^2 \setminus \Gamma_a$ which is an open set.



Source: Wikipedia

We are interested in $H_a = -\Delta_{\mathcal{D}}^{\mathcal{C}_a}$, the Dirichlet Laplacian in $L^2(\mathcal{C}_a)$. The value of a is not important: \mathcal{C}_a so changing it simply scales the spectrum.

The simplest case: an Archimedean waveguide



Let Γ_a be the Archimedean spiral in the plane with the slope $a > 0$, expressed in terms of the polar coordinates, $\Gamma_a = \{r = a\theta : \theta \geq 0\}$, and denote by \mathcal{C}_a its complement, $\mathcal{C}_a := \mathbb{R}^2 \setminus \Gamma_a$ which is an open set.



Source: Wikipedia

We are interested in $H_a = -\Delta_{\mathcal{D}}^{\mathcal{C}_a}$, the Dirichlet Laplacian in $L^2(\mathcal{C}_a)$. The value of a is not important: \mathcal{C}_a so changing it simply scales the spectrum.

The quadratic form associated with H_a looks in polar coordinates as

$$\begin{aligned} q_a : q_a[\psi] &= \int_0^\infty \int_{r_{\min}(\theta)}^{a\theta} \left[r \left| \frac{\partial \psi}{\partial r} \right|^2 + \frac{1}{r} \left| \frac{\partial \psi}{\partial \theta} \right|^2 \right] dr d\theta \\ &= \int_0^\infty \int_{r/a}^{(r+2\pi a)/a} \left[r \left| \frac{\partial \psi}{\partial r} \right|^2 + \frac{1}{r} \left| \frac{\partial \psi}{\partial \theta} \right|^2 \right] d\theta dr \end{aligned}$$

defined for all $\psi \in H^1(\Omega_a)$ satisfying Dirichlet condition at points of $\partial\Omega_a$ with $r > 0$ and such that $\lim_{r \rightarrow 0^+} \frac{\psi(r, \theta)}{\sin \frac{1}{2}\theta}$ exists being independent of θ .

Continuous spectrum of H_a



Theorem

We have $\sigma_{\text{ess}}(H_a) = [(2a)^{-2}, \infty)$. Furthermore, if I is an open interval away from $\mathcal{T} = \left\{ \left(\frac{n}{2a}\right)^2 : n = 1, 2, \dots \right\}$, then the spectrum of H_a in I is *purely absolutely continuous*.



P.E., M. Tater: Spectral properties of spiral-shaped quantum waveguides, *J. Phys. A: Math. Theor.* **53** (2020), 505303

Continuous spectrum of H_a



Theorem

We have $\sigma_{\text{ess}}(H_a) = [(2a)^{-2}, \infty)$. Furthermore, if I is an open interval away from $\mathcal{T} = \left\{ \left(\frac{n}{2a}\right)^2 : n = 1, 2, \dots \right\}$, then the spectrum of H_a in I is *purely absolutely continuous*.



P.E., M. Tater: Spectral properties of spiral-shaped quantum waveguides, *J. Phys. A: Math. Theor.* **53** (2020), 505303

Proof sketch: The *parallel coordinate* parametrization yields the first claim. Next we use *Mourre's commutator method* with the conjugate operator $A = -\frac{i}{2} \left(r \frac{\partial}{\partial r} + \frac{\partial}{\partial r} r \right)$ to \tilde{H}_a on Ω_a , the generator of the group of dilations of Ω_a in the direction parallel to the line $r = a\theta$

Continuous spectrum of H_a



Theorem

We have $\sigma_{\text{ess}}(H_a) = [(2a)^{-2}, \infty)$. Furthermore, if I is an open interval away from $\mathcal{T} = \left\{ \left(\frac{n}{2a}\right)^2 : n = 1, 2, \dots \right\}$, then the spectrum of H_a in I is *purely absolutely continuous*.



P.E., M. Tater: Spectral properties of spiral-shaped quantum waveguides, *J. Phys. A: Math. Theor.* **53** (2020), 505303

Proof sketch: The *parallel coordinate* parametrization yields the first claim. Next we use *Mourre's commutator method* with the conjugate operator $A = -\frac{i}{2} \left(r \frac{\partial}{\partial r} + \frac{\partial}{\partial r} r \right)$ to \tilde{H}_a on Ω_a , the generator of the group of dilations of Ω_a in the direction parallel to the line $r = a\theta$. We have

$$E_{\tilde{H}_a}(I)[\tilde{H}_a, iA]E_{\tilde{H}_a}(I) \geq -2 \frac{\partial^2}{\partial r^2} E_{\tilde{H}_a}(I) \geq \frac{1}{8} E_{\tilde{H}_a}(I);$$

the technical assumptions are satisfied and the bound contains no compact part, hence there are *no embedded eigenvalues* and the spectrum of \tilde{H}_a in the interval I is purely absolutely continuous. \square

Discrete spectrum?

The question about the existence of discrete spectrum below $(2a)^{-2}$ is equivalent to the positivity violation of the shifted quadratic form,

$$\psi \mapsto q_a[\psi] - \frac{1}{(2a)^2} \|\psi\|^2.$$



Discrete spectrum?



The question about the existence of discrete spectrum below $(2a)^{-2}$ is equivalent to the positivity violation of the shifted quadratic form,

$$\psi \mapsto q_a[\psi] - \frac{1}{(2a)^2} \|\psi\|^2.$$

Since $\psi(r, r/a) = \psi(r, (r + 2\pi a)/a) = 0$, we find easily

$$q_a[\psi] - \frac{1}{(2a)^2} \|\psi\|^2 \geq \rho_{(0,\infty)}[\psi],$$

where

$$\rho_{(\alpha,\beta)}[\psi] := \int_{\alpha}^{\beta} d\theta \int_{r_{\min}(\theta)}^{a\theta} \left[r \left| \frac{\partial \psi(r, \theta)}{\partial r} \right|^2 + \left(\frac{1}{4r} - \frac{r}{4a^2} \right) |\psi(r, \theta)|^2 \right] dr$$

Discrete spectrum?



The question about the existence of discrete spectrum below $(2a)^{-2}$ is equivalent to the positivity violation of the shifted quadratic form,

$$\psi \mapsto q_a[\psi] - \frac{1}{(2a)^2} \|\psi\|^2.$$

Since $\psi(r, r/a) = \psi(r, (r + 2\pi a)/a) = 0$, we find easily

$$q_a[\psi] - \frac{1}{(2a)^2} \|\psi\|^2 \geq p_{(0,\infty)}[\psi],$$

where

$$p_{(\alpha,\beta)}[\psi] := \int_{\alpha}^{\beta} d\theta \int_{r_{\min}(\theta)}^{a\theta} \left[r \left| \frac{\partial \psi(r, \theta)}{\partial r} \right|^2 + \left(\frac{1}{4r} - \frac{r}{4a^2} \right) |\psi(r, \theta)|^2 \right] dr$$

Using the Dirichlet conditions in the 'vertical' direction we can check that

$$p_{(\alpha,\beta)}[\psi] \geq 0 \quad \text{for any } 2\pi \leq \alpha < \beta \leq \infty,$$

and similarly, $p_{(\alpha,\beta)}[\psi] \geq 0$ for $\beta \leq \pi$

Discrete spectrum?



The question about the existence of discrete spectrum below $(2a)^{-2}$ is equivalent to the positivity violation of the shifted quadratic form,

$$\psi \mapsto q_a[\psi] - \frac{1}{(2a)^2} \|\psi\|^2.$$

Since $\psi(r, r/a) = \psi(r, (r + 2\pi a)/a) = 0$, we find easily

$$q_a[\psi] - \frac{1}{(2a)^2} \|\psi\|^2 \geq p_{(0,\infty)}[\psi],$$

where

$$p_{(\alpha,\beta)}[\psi] := \int_{\alpha}^{\beta} d\theta \int_{r_{\min}(\theta)}^{a\theta} \left[r \left| \frac{\partial \psi(r, \theta)}{\partial r} \right|^2 + \left(\frac{1}{4r} - \frac{r}{4a^2} \right) |\psi(r, \theta)|^2 \right] dr$$

Using the Dirichlet conditions in the 'vertical' direction we can check that

$$p_{(\alpha,\beta)}[\psi] \geq 0 \quad \text{for any } 2\pi \leq \alpha < \beta \leq \infty,$$

and similarly, $p_{(\alpha,\beta)}[\psi] \geq 0$ for $\beta \leq \pi$. Consequently, the only negative contribution can come from the interval $(\pi, 2\pi)$, in particular, that there can be *at most a finite number of bound states*

Discrete spectrum?



The question about the existence of discrete spectrum below $(2a)^{-2}$ is equivalent to the positivity violation of the shifted quadratic form,

$$\psi \mapsto q_a[\psi] - \frac{1}{(2a)^2} \|\psi\|^2.$$

Since $\psi(r, r/a) = \psi(r, (r + 2\pi a)/a) = 0$, we find easily

$$q_a[\psi] - \frac{1}{(2a)^2} \|\psi\|^2 \geq p_{(0,\infty)}[\psi],$$

where

$$p_{(\alpha,\beta)}[\psi] := \int_{\alpha}^{\beta} d\theta \int_{r_{\min}(\theta)}^{a\theta} \left[r \left| \frac{\partial \psi(r, \theta)}{\partial r} \right|^2 + \left(\frac{1}{4r} - \frac{r}{4a^2} \right) |\psi(r, \theta)|^2 \right] dr$$

Using the Dirichlet conditions in the 'vertical' direction we can check that

$$p_{(\alpha,\beta)}[\psi] \geq 0 \quad \text{for any } 2\pi \leq \alpha < \beta \leq \infty,$$

and similarly, $p_{(\alpha,\beta)}[\psi] \geq 0$ for $\beta \leq \pi$. Consequently, the only negative contribution can come from the interval $(\pi, 2\pi)$, in particular, that there can be *at most a finite number of bound states*. However, we are going to argue that the discrete spectrum is in fact *empty*.

Parallel coordinates



Let u be the distance from Γ_a along the inward pointing normal, then the points of \mathcal{C}_a can be parametrized (for $\theta > 2\pi$ at least) as

$$x_1(\theta, u) = a\theta \cos \theta - \frac{u}{\sqrt{1 + \theta^2}} (\sin \theta + \theta \cos \theta),$$

$$x_2(\theta, u) = a\theta \sin \theta + \frac{u}{\sqrt{1 + \theta^2}} (\cos \theta - \theta \sin \theta)$$

Parallel coordinates



Let u be the distance from Γ_a along the inward pointing normal, then the points of C_a can be parametrized (for $\theta > 2\pi$ at least) as

$$\begin{aligned}x_1(\theta, u) &= a\theta \cos \theta - \frac{u}{\sqrt{1 + \theta^2}} (\sin \theta + \theta \cos \theta), \\x_2(\theta, u) &= a\theta \sin \theta + \frac{u}{\sqrt{1 + \theta^2}} (\cos \theta - \theta \sin \theta)\end{aligned}$$

A natural counterpart to the variable u is the *arc length* of Γ_a given by

$$s(\theta) = a \int_0^\theta \sqrt{1 + \xi^2} d\xi = \frac{1}{2}a(\theta\sqrt{1 + \theta^2} + \ln(\theta + \sqrt{1 + \theta^2}))$$

which for large values of θ behaves as $s(\theta) = \frac{1}{2}a\theta^2 + \mathcal{O}(\ln \theta)$.

Parallel coordinates



Let u be the distance from Γ_a along the inward pointing normal, then the points of \mathcal{C}_a can be parametrized (for $\theta > 2\pi$ at least) as

$$\begin{aligned}x_1(\theta, u) &= a\theta \cos \theta - \frac{u}{\sqrt{1 + \theta^2}} (\sin \theta + \theta \cos \theta), \\x_2(\theta, u) &= a\theta \sin \theta + \frac{u}{\sqrt{1 + \theta^2}} (\cos \theta - \theta \sin \theta)\end{aligned}$$

A natural counterpart to the variable u is the *arc length* of Γ_a given by

$$s(\theta) = a \int_0^\theta \sqrt{1 + \xi^2} \, d\xi = \frac{1}{2}a(\theta\sqrt{1 + \theta^2} + \ln(\theta + \sqrt{1 + \theta^2}))$$

which for large values of θ behaves as $s(\theta) = \frac{1}{2}a\theta^2 + \mathcal{O}(\ln \theta)$.

Using it we can express the *curvature* of the spiral as

$$\kappa(\theta) = \frac{2 + \theta^2}{a(1 + \theta^2)^{3/2}} = \frac{1}{a\theta} + \mathcal{O}(\theta^{-2}) \quad \text{as } \theta \rightarrow \infty$$

which means that $\kappa(s) = \frac{1}{\sqrt{2as}} + \mathcal{O}(s^{-1})$ as $s \rightarrow \infty$.

What works against curvature-induced bounding?



In the strip $\Sigma_{a,\text{ext}} = \{(s, u) : s > s(2\pi), u \in (0, d(s))\}$ we can then pass to a unitarily equivalent operator acting as

$$\hat{H}_{a,\text{ext}}\psi = -\frac{\partial}{\partial s}(1 - u\kappa(s))^{-2}\frac{\partial\psi}{\partial s}(s, u) - \frac{\partial^2\psi}{\partial u^2}(s, u) + V(s, u)\psi(s, u),$$

where

$$V(s, u) := -\frac{\kappa(s)^2}{4(1 - u\kappa(s))^2} - \frac{u\ddot{\kappa}(s)}{2(1 - u\kappa(s))^3} - \frac{5}{4}\frac{u^2\dot{\kappa}(s)^2}{(1 - u\kappa(s))^4},$$

with an appropriate boundary condition at $s = s(2\pi)$.

What works against curvature-induced bounding?



In the strip $\Sigma_{a,\text{ext}} = \{(s, u) : s > s(2\pi), u \in (0, d(s))\}$ we can then pass to a unitarily equivalent operator acting as

$$\hat{H}_{a,\text{ext}}\psi = -\frac{\partial}{\partial s}(1 - u\kappa(s))^{-2}\frac{\partial\psi}{\partial s}(s, u) - \frac{\partial^2\psi}{\partial u^2}(s, u) + V(s, u)\psi(s, u),$$

where

$$V(s, u) := -\frac{\kappa(s)^2}{4(1 - u\kappa(s))^2} - \frac{u\ddot{\kappa}(s)}{2(1 - u\kappa(s))^3} - \frac{5}{4}\frac{u^2\dot{\kappa}(s)^2}{(1 - u\kappa(s))^4},$$

with an appropriate boundary condition at $s = s(2\pi)$.

The point is that while the *radial* width of the Archimedes spiral is constant, the 'true', *perpendicular* one, denoted as $d(s)$, is *smaller than $2\pi a$* and only *asymptotically* constant: we have

$$\frac{\pi^2}{d(s)^2} - \frac{1}{4a^2} + V(s, u) = \frac{\pi - u}{2a^2\theta^3} + \mathcal{O}(\theta^{-4}),$$

and as a result, the contributions to the effective potential cancel in the leading order as $\theta \rightarrow \infty$ *eliminating thus the curvature-induced attraction*.

A variation: spiral waveguide with a cavity



Let us *'erase' a part of the Dirichlet boundary*, that is, we impose the condition on the 'cut' Archimedean spiral $\Gamma_{a,\beta}$ for some $\beta > 0$, where $\Gamma_{a,\beta} = \{r = a\theta : \theta \geq \beta\}$. The particle thus 'lives' in $\mathcal{C}_{a,\beta} := \mathbb{R}^2 \setminus \Gamma_{a,\beta}$ and its Hamiltonian, modulo unimportant physical constants, is

$$H_{a,\beta} = -\Delta_{\mathcal{D}}^{\mathcal{C}_{a,\beta}},$$

the Dirichlet Laplacian in $L^2(\mathcal{C}_{a,\beta})$

A variation: spiral waveguide with a cavity



Let us *'erase' a part of the Dirichlet boundary*, that is, we impose the condition on the 'cut' Archimedean spiral $\Gamma_{a,\beta}$ for some $\beta > 0$, where $\Gamma_{a,\beta} = \{r = a\theta : \theta \geq \beta\}$. The particle thus 'lives' in $\mathcal{C}_{a,\beta} := \mathbb{R}^2 \setminus \Gamma_{a,\beta}$ and its Hamiltonian, modulo unimportant physical constants, is

$$H_{a,\beta} = -\Delta_{\mathcal{D}}^{\mathcal{C}_{a,\beta}},$$

the Dirichlet Laplacian in $L^2(\mathcal{C}_{a,\beta})$. Obviously, we have

$$\sigma_{\text{ess}}(H_{a,\beta}) = [(2a)^{-2}, \infty).$$

A variation: spiral waveguide with a cavity



Let us *'erase' a part of the Dirichlet boundary*, that is, we impose the condition on the 'cut' Archimedean spiral $\Gamma_{a,\beta}$ for some $\beta > 0$, where $\Gamma_{a,\beta} = \{r = a\theta : \theta \geq \beta\}$. The particle thus 'lives' in $\mathcal{C}_{a,\beta} := \mathbb{R}^2 \setminus \Gamma_{a,\beta}$ and its Hamiltonian, modulo unimportant physical constants, is

$$H_{a,\beta} = -\Delta_D^{\mathcal{C}_{a,\beta}},$$

the Dirichlet Laplacian in $L^2(\mathcal{C}_{a,\beta})$. Obviously, we have

$$\sigma_{\text{ess}}(H_{a,\beta}) = [(2a)^{-2}, \infty).$$

By bracketing, the discrete spectrum is nonempty for β large enough:

Proposition

There is a critical $\beta_1 = 2j_{0,1} \approx 4.805 \approx 1.531\pi$ such that $\sigma_{\text{disc}}(H_{a,\beta}) \neq \emptyset$ holds for all $\beta > \beta_1$

A variation: spiral waveguide with a cavity



Let us *'erase' a part of the Dirichlet boundary*, that is, we impose the condition on the 'cut' Archimedean spiral $\Gamma_{a,\beta}$ for some $\beta > 0$, where $\Gamma_{a,\beta} = \{r = a\theta : \theta \geq \beta\}$. The particle thus 'lives' in $\mathcal{C}_{a,\beta} := \mathbb{R}^2 \setminus \Gamma_{a,\beta}$ and its Hamiltonian, modulo unimportant physical constants, is

$$H_{a,\beta} = -\Delta_D^{\mathcal{C}_{a,\beta}},$$

the Dirichlet Laplacian in $L^2(\mathcal{C}_{a,\beta})$. Obviously, we have

$$\sigma_{\text{ess}}(H_{a,\beta}) = [(2a)^{-2}, \infty).$$

By bracketing, the discrete spectrum is nonempty for β large enough:

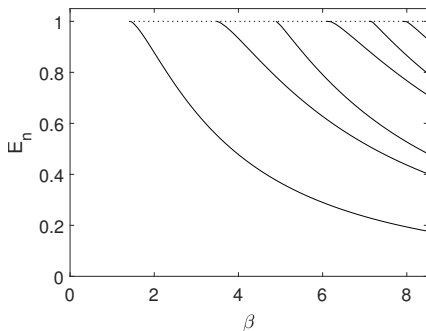
Proposition

There is a critical $\beta_1 = 2j_{0,1} \approx 4.805 \approx 1.531\pi$ such that $\sigma_{\text{disc}}(H_{a,\beta}) \neq \emptyset$ holds for all $\beta > \beta_1$. Furthermore, let $\mathcal{B} = \{\beta_j\}_{j=1}^\infty$ be the sequence $\mathcal{B} = \{2j_{0,1}, 2j_{1,1}, 2j_{1,1}, 2j_{2,1}, 2j_{2,1}, 2j_{0,2}, 2j_{1,2}, 2j_{1,2}, \dots\}$ composed of zeros of Bessel functions J_n , $n = 0, 1, \dots$, then for *any* $\beta > \beta_j$ the operator $H_{a,\beta}$ has *at least* j eigenvalues, the multiplicity taken into account.

Eigenvalues



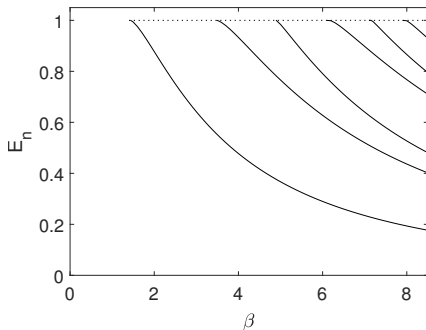
One can solve the problem numerically using *FEM technique*; here is how the eigenvalues of $H_{1/2,\beta}$ depend on the angle β :



Eigenvalues



One can solve the problem numerically using *FEM technique*; here is how the eigenvalues of $H_{1/2,\beta}$ depend on the angle β :

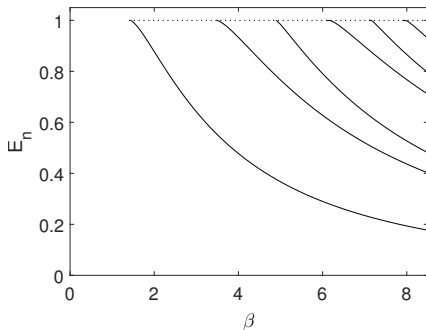


As expected, they are monotonously decreasing functions. We also can identify the critical angle at which the first eigenvalue appears to be $\beta_1 \approx 1.43 \approx 0.455\pi$, a much smaller value than the above sufficient condition

Eigenvalues



One can solve the problem numerically using *FEM technique*; here is how the eigenvalues of $H_{1/2,\beta}$ depend on the angle β :



As expected, they are monotonously decreasing functions. We also can identify the critical angle at which the first eigenvalue appears to be $\beta_1 \approx 1.43 \approx 0.455\pi$, a much smaller value than the above sufficient condition; what is more important, it provides the *indication that the discrete spectrum of the 'full' Archimedean spiral region is void.*

Eigenfunctions

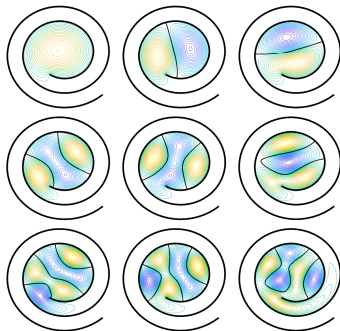


Figure: The first nine eigenfunctions of $H_{1/2, 21/2}$ shown through their horizontal levels. The corresponding energies are 0.1280, 0.2969, 0.3456, 0.5312, 0.5811, 0.6825, 0.8266, 0.8852, and 0.9768, respectively.

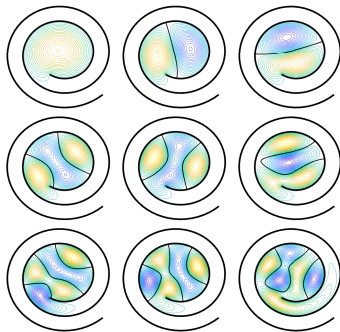


Figure: The first nine eigenfunctions of $H_{1/2,21/2}$ shown through their horizontal levels. The corresponding energies are 0.1280, 0.2969, 0.3456, 0.5312, 0.5811, 0.6825, 0.8266, 0.8852, and 0.9768, respectively.

The results agree with the Courant nodal domain theorem; the nodal lines are situated in the cavity only which, as well the finiteness of the spectrum, corresponds nicely to the observation that the part of $\mathcal{C}_{a,\beta}$ referring to the angles $\theta > \max\{2\pi, \beta_1\}$ is a *classically forbidden zone*.

A variation: multi-arm Archimedean waveguide



Let Γ_a^m be the union of m Archimedean spirals with slope $a > 0$ and an angular shift, $\Gamma_a^m = \{r = a(\theta - \frac{2\pi j}{m}) : \theta \geq \frac{2\pi j}{m}, j = 0, \dots, m-1\}$.

As before we consider its complement $C_a^m := \mathbb{R}^2 \setminus \Gamma_a^m$ and the operator

$$H_a = -\Delta_D^{C_a^m}.$$

A variation: multi-arm Archimedean waveguide



Let Γ_a^m be the union of m Archimedean spirals with slope $a > 0$ and an angular shift, $\Gamma_a^m = \{r = a(\theta - \frac{2\pi j}{m}) : \theta \geq \frac{2\pi j}{m}, j = 0, \dots, m-1\}$.

As before we consider its complement $\mathcal{C}_a^m := \mathbb{R}^2 \setminus \Gamma_a^m$ and the operator

$$H_a = -\Delta_{\mathcal{C}_a^m}.$$

The analysis is similar, but there is a difference coming from regularity of the boundary. For $m = 2$ the set \mathcal{C}_a^2 consists of two connected components and has a *smooth boundary*, for $m \geq 3$ it consists of m connected components separated by the branches of Γ_a^m , each of them has an angle at the origin of coordinates which is $\frac{2\pi}{m}$, that is, *convex*; this means that for $m \geq 2$ the *singular component is missing*.

A variation: multi-arm Archimedean waveguide



Let Γ_a^m be the union of m Archimedean spirals with slope $a > 0$ and an angular shift, $\Gamma_a^m = \{r = a(\theta - \frac{2\pi j}{m}) : \theta \geq \frac{2\pi j}{m}, j = 0, \dots, m-1\}$.

As before we consider its complement $\mathcal{C}_a^m := \mathbb{R}^2 \setminus \Gamma_a^m$ and the operator

$$H_a = -\Delta_D^{\mathcal{C}_a^m}.$$

The analysis is similar, but there is a difference coming from regularity of the boundary. For $m = 2$ the set \mathcal{C}_a^2 consists of two connected components and has a *smooth boundary*, for $m \geq 3$ it consists of m connected components separated by the branches of Γ_a^m , each of them has an angle at the origin of coordinates which is $\frac{2\pi}{m}$, that is, *convex*; this means that for $m \geq 2$ the *singular component is missing*.

It is sufficient to consider one connected component of \mathcal{C}_a^m only, i.e. the operator $\tilde{H}_a^m = -\frac{\partial^2 f}{\partial r^2} - \frac{1}{r^2} \frac{\partial^2 f}{\partial \theta^2} - \frac{1}{4r^2}$ referring to the skewed strip

$$\Omega_a^m := \{(r, \theta) : r \in (r_{\min}^m(\theta), a\theta), \theta > 0\},$$

where $r_{\min}^m(\theta) := \max\{0, a(\theta - \frac{2\pi}{m})\}$ with $D(H_a^m) = \mathcal{H}^2(\Omega_a^m) \cap \mathcal{H}_0^1(\Omega_a^m)$.

Spectrum of multi-arm spiral region



Proposition

$\sigma(H_a^m) = [(\frac{m}{2a})^2, \infty)$ for any natural $m \geq 2$. The spectrum is *absolutely continuous* outside $\mathcal{T}_m = \{(\frac{mn}{2a})^2 : n = 1, 2, \dots\}$ and its multiplicity is divisible by m .

Spectrum of multi-arm spiral region



Proposition

$\sigma(H_a^m) = [(\frac{m}{2a})^2, \infty)$ for any natural $m \geq 2$. The spectrum is *absolutely continuous* outside $\mathcal{T}_m = \{(\frac{mn}{2a})^2 : n = 1, 2, \dots\}$ and its multiplicity is divisible by m .

Proof sketch: The multiplicity claim is obvious. The above arguments used to determine the essential spectrum and to prove its absolute continuity outside the thresholds modify easily.

Spectrum of multi-arm spiral region



Proposition

$\sigma(H_a^m) = [(\frac{m}{2a})^2, \infty)$ for any natural $m \geq 2$. The spectrum is *absolutely continuous* outside $\mathcal{T}_m = \{(\frac{mn}{2a})^2 : n = 1, 2, \dots\}$ and its multiplicity is divisible by m .

Proof sketch: The multiplicity claim is obvious. The above arguments used to determine the essential spectrum and to prove its absolute continuity outside the thresholds modify easily.

Furthermore, *the discrete spectrum is void*. Indeed, since the domain is now 'pure Sobolev', the bottom part, $r = 0$, of the skewed strip supports Dirichlet condition. This means that

$$p_{(\alpha, \beta)}^m[\psi] \geq 0 \quad \text{now for any } 0 \leq \alpha < \beta \leq \infty$$

so that $q_a^m[\psi] - \left(\frac{m}{2a}\right)^2 \|\psi\|^2 \geq p_{(0, \infty)}^m[\psi] \geq 0$ for any $\psi \in \text{dom}[q_a^m]$. □

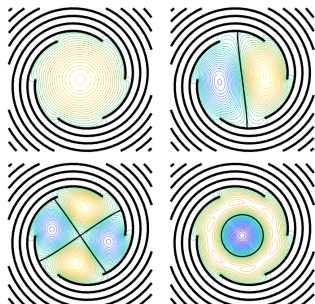


Figure: The j th eigenfunction, $j = 1, 2, 4, 6$, of $H_{3,2\pi}^6$, the corresponding energies are 0.1296, 0.3282, 0.5871, and 0.6783, respectively.

Here we plot result for a six-arm spiral region with the central cavity. As expected, with the growing m the eigenfunctions – with the possible exception of states close to the threshold – become similar to those of the Dirichlet Laplacian in a disc; it is instructive to compare the nodal lines to those of the single arm region shown above.

General spirals



There are many spirals beyond the Archimedean case, for instance



logarithmic

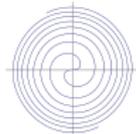
General spirals



There are many spirals beyond the Archimedean case, for instance



logarithmic



Fermat

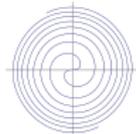
General spirals



There are many spirals beyond the Archimedean case, for instance



logarithmic



Fermat



Poincaré

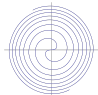
General spirals



There are many spirals beyond the Archimedean case, for instance



logarithmic



Fermat



Poincaré



Atzema

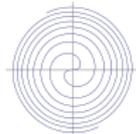
General spirals



There are many spirals beyond the Archimedean case, for instance



logarithmic



Fermat



Poincaré



Atzema



Fibonacci

General spirals



There are many spirals beyond the Archimedean case, for instance



logarithmic



Fermat



Poincaré



Atzema



Fibonacci



Theodorus

Source: Wikipedia

A spiral curve Γ can be described in polar coordinates as the family of points $(r(\theta), \theta)$, where $r(\cdot)$ is a given increasing function. Let us assume that $r(\cdot)$ is a *C^2 -smooth function* excluding thus well-known curves such as *Fibonacci spiral*, *spiral of Theodorus*, etc.

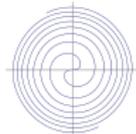
General spirals



There are many spirals beyond the Archimedean case, for instance



logarithmic



Fermat



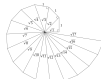
Poincot



Atzema



Fibonacci



Theodorus

Source: Wikipedia

A spiral curve Γ can be described in polar coordinates as the family of points $(r(\theta), \theta)$, where $r(\cdot)$ is a given increasing function. Let us assume that $r(\cdot)$ is a *C^2 -smooth function* excluding thus well-known curves such as *Fibonacci spiral*, *spiral of Theodorus*, etc.

Remarks: (i) The spirals considered are semi-infinite $r : \mathbb{R}_+ \rightarrow \mathbb{R}_+$. One can also consider '*fully infinite spirals*' for which $r : \mathbb{R} \rightarrow \mathbb{R}_+$.

(ii) *A warning:* It matters that the boundary is *Dirichlet*, for *Neumann* the spectral properties can be completely different as the well-known Simon's example, in which $r(\theta) = \frac{3}{4} + \frac{1}{2\pi} \arctan \theta$, shows.



B. Simon: The Neumann Laplacian of a jelly roll, *Proc. AMS* 114 (1992), 783–785.

General spirals



The monotonicity of r means that Γ does not intersect itself, in other words, the *width function* $a : a(\theta) = \frac{1}{2\pi} (r(\theta) - r(\theta - 2\pi))$ is positive for any $\theta \geq 2\pi$. The 'inward' coil width is $2\pi a(\theta)$; we make this choice with the correspondence to the Archimedean case in mind).

General spirals



The monotonicity of r means that Γ does not intersect itself, in other words, the *width function* $a : a(\theta) = \frac{1}{2\pi} (r(\theta) - r(\theta - 2\pi))$ is positive for any $\theta \geq 2\pi$. The 'inward' coil width is $2\pi a(\theta)$; we make this choice with the correspondence to the Archimedean case in mind).

As before we denote $\mathcal{C} := \mathbb{R}^2 \setminus \Gamma$ and ask about spectral properties of the Dirichlet Laplacian $H_r = -\Delta_{\mathcal{D}}^{\mathcal{C}}$ in $L^2(\mathcal{C})$.

General spirals



The monotonicity of r means that Γ does not intersect itself, in other words, the *width function* $a : a(\theta) = \frac{1}{2\pi} (r(\theta) - r(\theta - 2\pi))$ is positive for any $\theta \geq 2\pi$. The 'inward' coil width is $2\pi a(\theta)$; we make this choice with the correspondence to the Archimedean case in mind).

As before we denote $\mathcal{C} := \mathbb{R}^2 \setminus \Gamma$ and ask about spectral properties of the Dirichlet Laplacian $H_r = -\Delta_{\mathcal{C}}^D$ in $L^2(\mathcal{C})$.

Multiarm-arm spirals are similarly described by an m -tuple of increasing functions $r_j : [\theta_j, \infty) \rightarrow \mathbb{R}_+$, $j = 0, 1, \dots, m-1$ referring to angles $0 = \theta_0 < \theta_1 < \dots < \theta_{m-1} < 2\pi$ satisfying

$$a_j(\theta) := \frac{1}{2\pi} (r_j(\theta) - r_{j+1}(\theta)) > 0 \quad \text{for } \theta \geq \theta_j$$

General spirals



The monotonicity of r means that Γ does not intersect itself, in other words, the *width function* $a : a(\theta) = \frac{1}{2\pi} (r(\theta) - r(\theta - 2\pi))$ is positive for any $\theta \geq 2\pi$. The 'inward' coil width is $2\pi a(\theta)$; we make this choice with the correspondence to the Archimedean case in mind).

As before we denote $\mathcal{C} := \mathbb{R}^2 \setminus \Gamma$ and ask about spectral properties of the Dirichlet Laplacian $H_r = -\Delta_{\mathcal{C}}^D$ in $L^2(\mathcal{C})$.

Multiarm-arm spirals are similarly described by an m -tuple of increasing functions $r_j : [\theta_j, \infty) \rightarrow \mathbb{R}_+$, $j = 0, 1, \dots, m-1$ referring to angles $0 = \theta_0 < \theta_1 < \dots < \theta_{m-1} < 2\pi$ satisfying

$$a_j(\theta) := \frac{1}{2\pi} (r_j(\theta) - r_{j+1}(\theta)) > 0 \quad \text{for } \theta \geq \theta_j$$

Note that a two-arm spiral can also be alternatively described by means of a function $r : \mathbb{R} \rightarrow \mathbb{R}$ such that $\pm r(\theta) > 0$ for $\pm\theta > 0$ if we interpret *negative radii* as describing vectors rotated by π .

Types of general spirals



Asymptotic properties of the width function are decisive. We call a spiral-shaped region \mathcal{C} *simple* if the function $a(\cdot)$ is monotonous (or monotonous on both the halflines \mathbb{R}_{\pm}).

Types of general spirals



Asymptotic properties of the width function are decisive. We call a spiral-shaped region \mathcal{C} *simple* if the function $a(\cdot)$ is monotonous (or monotonous on both the halflines \mathbb{R}_{\pm}).

A simple \mathcal{C} is called *expanding* and *shrinking* if $a(\cdot)$ is increasing and decreasing, respectively, for $\theta \geq 0$

Types of general spirals



Asymptotic properties of the width function are decisive. We call a spiral-shaped region \mathcal{C} *simple* if the function $a(\cdot)$ is monotonous (or monotonous on both the halflines \mathbb{R}_{\pm}).

A simple \mathcal{C} is called *expanding* and *shrinking* if $a(\cdot)$ is increasing and decreasing, respectively, for $\theta \geq 0$; these qualifications are labeled correspondingly as *strict* if $\lim_{\theta \rightarrow \infty} a(\theta) = \infty$ and $\lim_{\theta \rightarrow \infty} a(\theta) = 0$.

Types of general spirals



Asymptotic properties of the width function are decisive. We call a spiral-shaped region \mathcal{C} *simple* if the function $a(\cdot)$ is monotonous (or monotonous on both the halflines \mathbb{R}_{\pm}).

A simple \mathcal{C} is called *expanding* and *shrinking* if $a(\cdot)$ is increasing and decreasing, respectively, for $\theta \geq 0$; these qualifications are labeled correspondingly as *strict* if $\lim_{\theta \rightarrow \infty} a(\theta) = \infty$ and $\lim_{\theta \rightarrow \infty} a(\theta) = 0$.

A spiral-shaped region is called *asymptotically Archimedean* if there is an $a_0 \in \mathbb{R}$ such that $\lim_{\theta \rightarrow \infty} a(\theta) = a_0$, for multi-arm spirals this means finite limits of all the a_j .

Types of general spirals



Asymptotic properties of the width function are decisive. We call a spiral-shaped region \mathcal{C} *simple* if the function $a(\cdot)$ is monotonous (or monotonous on both the halflines \mathbb{R}_{\pm}).

A simple \mathcal{C} is called *expanding* and *shrinking* if $a(\cdot)$ is increasing and decreasing, respectively, for $\theta \geq 0$; these qualifications are labeled correspondingly as *strict* if $\lim_{\theta \rightarrow \infty} a(\theta) = \infty$ and $\lim_{\theta \rightarrow \infty} a(\theta) = 0$.

A spiral-shaped region is called *asymptotically Archimedean* if there is an $a_0 \in \mathbb{R}$ such that $\lim_{\theta \rightarrow \infty} a(\theta) = a_0$, for multi-arm spirals this means finite limits of all the a_j .

A region \mathcal{C} is obviously unbounded iff $\lim_{\theta \rightarrow \infty} r(\theta) = \infty$. If the limit is finite, $\lim_{\theta \rightarrow \infty} r(\theta) = R$, the closure $\bar{\mathcal{C}}$ is contained in the circle of radius R , it may or may not be simply connected as the example of *Simon's jelly roll* mentioned above shows (and the Neumann Laplacian spectrum in this region is *purely continuous*).

Description of general spiral regions



The Hamiltonian domain is $D(H_r) = \mathcal{H}^2(\Omega_r) \cap \mathcal{H}_0^1(\Omega_r) \oplus \mathbb{C}(\psi_{\text{sing}})$, with the singular element missing if the boundary is convex around the origin. In polar coordinates H_r is an operator on a *skewed strip*, now of a generally *nonconstant width*

Description of general spiral regions



The Hamiltonian domain is $D(H_r) = \mathcal{H}^2(\Omega_r) \cap \mathcal{H}_0^1(\Omega_r) \oplus \mathbb{C}(\psi_{\text{sing}})$, with the singular element missing if the boundary is convex around the origin. In polar coordinates H_r is an operator on a *skewed strip*, now of a generally *nonconstant width*. The quadratic form associated with H_r is

$$\begin{aligned} q_r : q_r[\psi] &= \int_0^\infty \int_{r_{\min}(\theta)}^{r(\theta)} \left[r \left| \frac{\partial \psi}{\partial r} \right|^2 + \frac{1}{r} \left| \frac{\partial \psi}{\partial \theta} \right|^2 \right] dr d\theta \\ &= \int_0^\infty \int_{\theta^{-1}(r)}^{\theta^{-1}(r)+2\pi} \left[r \left| \frac{\partial \psi}{\partial r} \right|^2 + \frac{1}{r} \left| \frac{\partial \psi}{\partial \theta} \right|^2 \right] d\theta dr \end{aligned}$$

where $\theta^{-1}(\cdot)$ is the pull-back of the function $r(\cdot)$; its domain consists of function $\psi \in H^1(\Omega_r)$ satisfying appropriate conditions at $\partial\Omega_a$.

Description of general spiral regions



The Hamiltonian domain is $D(H_r) = \mathcal{H}^2(\Omega_r) \cap \mathcal{H}_0^1(\Omega_r) \oplus \mathbb{C}(\psi_{\text{sing}})$, with the singular element missing if the boundary is convex around the origin. In polar coordinates H_r is an operator on a *skewed strip*, now of a generally *nonconstant width*. The quadratic form associated with H_r is

$$\begin{aligned} q_r : q_r[\psi] &= \int_0^\infty \int_{r_{\min}(\theta)}^{r(\theta)} \left[r \left| \frac{\partial \psi}{\partial r} \right|^2 + \frac{1}{r} \left| \frac{\partial \psi}{\partial \theta} \right|^2 \right] dr d\theta \\ &= \int_0^\infty \int_{\theta^{-1}(r)}^{\theta^{-1}(r)+2\pi} \left[r \left| \frac{\partial \psi}{\partial r} \right|^2 + \frac{1}{r} \left| \frac{\partial \psi}{\partial \theta} \right|^2 \right] d\theta dr \end{aligned}$$

where $\theta^{-1}(\cdot)$ is the pull-back of the function $r(\cdot)$; its domain consists of function $\psi \in H^1(\Omega_r)$ satisfying appropriate conditions at $\partial\Omega_a$.

We can also express the *arc length* of Γ and its *curvature*; they are

$$s(\theta) = \int_0^\theta \sqrt{\dot{r}(\xi)^2 + r(\xi)^2} d\xi \quad \text{and} \quad \kappa(\theta) = \frac{r(\theta)^2 + 2\dot{r}(\theta)^2 - r(\theta)\ddot{r}(\theta)}{(r(\theta)^2 + \dot{r}(\theta)^2)^{3/2}}.$$

Strictly expanding spiral regions



In contrast to the Archimedean case, it may not be possible to amend the arclength with the orthogonal coordinate u to parametrize \mathcal{C}_r by

$$x_1(\theta, u) = r(\theta) \cos \theta - \frac{u}{\sqrt{\dot{r}(\theta)^2 + r(\theta)^2}} (\dot{r}(\theta) \sin \theta + r(\theta) \cos \theta),$$
$$x_2(\theta, u) = r(\theta) \sin \theta + \frac{u}{\sqrt{\dot{r}(\theta)^2 + r(\theta)^2}} (\dot{r}(\theta) \cos \theta - r(\theta) \sin \theta).$$

The reason is that for strictly expanding spirals the inward normal at a point may not intersect the previous spiral coil; it is easy to check that in the examples of a *logarithmic spiral*, $r(\theta) = a e^{k\theta}$ with $a, k > 0$, or *hyperbolic spiral*, $r(\theta) = a\theta^{-1}$.

Strictly expanding spiral regions



In contrast to the Archimedean case, it may not be possible to amend the arclength with the orthogonal coordinate u to parametrize \mathcal{C}_r by

$$x_1(\theta, u) = r(\theta) \cos \theta - \frac{u}{\sqrt{\dot{r}(\theta)^2 + r(\theta)^2}} (\dot{r}(\theta) \sin \theta + r(\theta) \cos \theta),$$
$$x_2(\theta, u) = r(\theta) \sin \theta + \frac{u}{\sqrt{\dot{r}(\theta)^2 + r(\theta)^2}} (\dot{r}(\theta) \cos \theta - r(\theta) \sin \theta).$$

The reason is that for strictly expanding spirals the inward normal at a point may not intersect the previous spiral coil; it is easy to check that in the examples of a *logarithmic spiral*, $r(\theta) = a e^{k\theta}$ with $a, k > 0$, or *hyperbolic spiral*, $r(\theta) = a\theta^{-1}$.

Fortunately, some properties of H_r can be derived without the use of the locally orthogonal system. Using suitable Weyl sequences one can prove the following claim:

Proposition

$\sigma(H_r) = \sigma_{\text{ess}}(H_r) = [0, \infty)$ holds if \mathcal{C} is *simple and strictly expanding*.

Strictly shrinking spiral regions



On the other hand, parallel coordinates *can be used*, possibly outside a compact region, if \mathcal{C} is generated by a shrinking or an asymptotically Archimedean spirals.

Strictly shrinking spiral regions



On the other hand, parallel coordinates *can be used*, possibly outside a compact region, if \mathcal{C} is generated by a shrinking or an asymptotically Archimedean spirals.

We combine bracketing with the unitarily equivalent form of the operator in parallel coordinates,

$$\hat{H}_{\text{nc}}^{\text{D}} \geq -\frac{\partial}{\partial s} (1 - u\kappa(s))^{-2} \frac{\partial}{\partial s} + \frac{\pi^2}{d(s)^2} + V(s, u)$$

and similarly for $\hat{H}_{\text{nc}}^{\text{N}}$. Since $d(s) \rightarrow 0$ as $s \rightarrow \infty$ holds is a strictly shrinking region, the sum of the two last term explodes in the limit, and in the standard way we can check the following claim:

Proposition

If \mathcal{C} is simple and strictly shrinking, the spectrum of H_r is purely discrete.

Example: Fermat spiral

For *Fermat spiral*, $r(\theta)^2 = b^2\theta$, we have $a(\theta) = \frac{1}{2}b\theta^{-1/2} + \mathcal{O}(\theta^{-3/2})$
so the spectrum is discrete



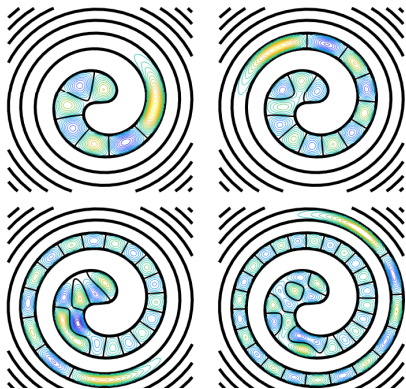
Example: Fermat spiral

For *Fermat spiral*, $r(\theta)^2 = b^2\theta$, we have $a(\theta) = \frac{1}{2}b\theta^{-1/2} + \mathcal{O}(\theta^{-3/2})$ so the spectrum is discrete. Moreover, apart from the central region the eigenfunctions have a quasi-one-dimensional character, as illustrated for $b = 1$ and eigenfunctions corresponding to the eigenvalues, $E_7 = 19.5462$, $E_{15} = 28.3118$, $E_{27} = 38.8062$, and $E_{42} = 48.8367$.



Example: Fermat spiral

For *Fermat spiral*, $r(\theta)^2 = b^2\theta$, we have $a(\theta) = \frac{1}{2}b\theta^{-1/2} + \mathcal{O}(\theta^{-3/2})$ so the spectrum is discrete. Moreover, apart from the central region the eigenfunctions have a quasi-one-dimensional character, as illustrated for $b = 1$ and eigenfunctions corresponding to the eigenvalues, $E_7 = 19.5462$, $E_{15} = 28.3118$, $E_{27} = 38.8062$, and $E_{42} = 48.8367$.



Fermat spiral region: number of eigenvalues

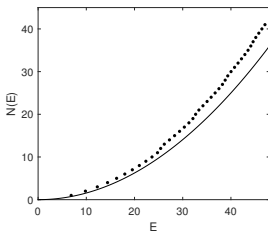


The dominant contribution to the eigenvalue count comes from the transverse confinement potential $v(\theta) = \left(\frac{\pi}{d(\theta)}\right)^2$. For Fermat spiral region this leads to the asymptotics $N(E) \approx \frac{1}{64} b^4 E^2$ as $E \rightarrow \infty$.

Fermat spiral region: number of eigenvalues



The dominant contribution to the eigenvalue count comes from the transverse confinement potential $v(\theta) = \left(\frac{\pi}{d(\theta)}\right)^2$. For Fermat spiral region this leads to the asymptotics $N(E) \approx \frac{1}{64} b^4 E^2$ as $E \rightarrow \infty$.



However, a numerical evaluation of the spectrum shows a significant excess that can be naturally attributed to the geometry-related effects, see also

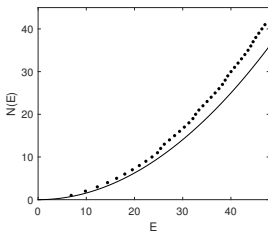


M. van den Berg, E.B. Davies: Heat flow out of regions in \mathbb{R}^m , *Math. Z.* **202** (1989), 463–482.

Fermat spiral region: number of eigenvalues



The dominant contribution to the eigenvalue count comes from the transverse confinement potential $v(\theta) = \left(\frac{\pi}{d(\theta)}\right)^2$. For Fermat spiral region this leads to the asymptotics $N(E) \approx \frac{1}{64} b^4 E^2$ as $E \rightarrow \infty$.



However, a numerical evaluation of the spectrum shows a significant excess that can be naturally attributed to the geometry-related effects, see also



M. van den Berg, E.B. Davies: Heat flow out of regions in \mathbb{R}^m , *Math. Z.* **202** (1989), 463–482.

On the other hand, one can derive a *Lieb-Thirring-type inequality* which shows that *asymptotically* it is only the spiral width here that matters.



D. Barseghyan, P.E.: Spectral estimates for Dirichlet Laplacian on spiral-shaped regions, *J. Spect. Theory*, to appear; arXiv:2206.14058

Asymptotically Archimedean regions



Between the above discussed extremes the situation is much more interesting. Modifying the argument in the Archimedean case we get

Proposition

If the spiral Γ is *asymptotically Archimedean* with $\lim_{\theta \rightarrow \infty} a(\theta) = a_0$, we have $\sigma_{\text{ess}}(H_r) = [(2a_0)^{-2}, \infty)$. In the case of a *multi-arm region* with $\lim_{\theta \rightarrow \infty} a_j(\theta) = a_{0,j}$, the essential spectrum is $[(2\bar{a})^{-2}, \infty)$, where $\bar{a} := \max_{0 \leq j \leq m-1} a_{0,j}$.

Asymptotically Archimedean regions



Between the above discussed extremes the situation is much more interesting. Modifying the argument in the Archimedean case we get

Proposition

If the spiral Γ is *asymptotically Archimedean* with $\lim_{\theta \rightarrow \infty} a(\theta) = a_0$, we have $\sigma_{\text{ess}}(H_r) = [(2a_0)^{-2}, \infty)$. In the case of a *multi-arm region* with $\lim_{\theta \rightarrow \infty} a_j(\theta) = a_{0,j}$, the essential spectrum is $[(2\bar{a})^{-2}, \infty)$, where $\bar{a} := \max_{0 \leq j \leq m-1} a_{0,j}$.

The question about the discrete spectrum is more subtle and the type of asymptotics is decisive. Let us consider the spiral

$$r(\theta) = a_0\theta + b_0 - \rho(\theta),$$

where $\rho(\cdot)$ is a positive function such that, $\lim_{\theta \rightarrow \infty} \rho(\theta) = 0$; for the sake of definiteness we restrict our attention to functions satisfying

$$\dot{\rho}(\theta) = -\frac{c}{\theta^\gamma} + \mathcal{O}(\theta^{-\gamma-1}) \quad \text{as } \theta \rightarrow \infty \quad \text{with } 1 < \gamma < 3.$$

Theorem

For the described $r(\cdot)$, $\#\sigma_{\text{disc}}(H_r) = \infty$ holds for any $c > 0$.



P.E., M. Tater: Spectral properties of spiral-shaped quantum waveguides, *J. Phys. A: Math. Theor.* **53** (2020), 505303

Theorem

For the described $r(\cdot)$, $\#\sigma_{\text{disc}}(H_r) = \infty$ holds for any $c > 0$.



P.E., M. Tater: Spectral properties of spiral-shaped quantum waveguides, *J. Phys. A: Math. Theor.* **53** (2020), 505303

Proof sketch: By a variational argument, using the trial functions $\psi_{0,\lambda}$ with mollifier μ that gave the essential spectrum in the Archimedean case. After a straightforward computation we get for the shifted quadratic form

$$p[\psi_{0,\lambda}] < \lambda \frac{4\pi}{a_0} \|\mu\|^2 - \left(\frac{4\pi^2 c}{a_0^4} \left(\frac{a_0}{4} \right)^{\gamma/2} \lambda^{(\gamma-2)/2} + \mathcal{O}(\lambda^{(\gamma'-2)/2}) \right) \|\mu\|^2,$$

where the right-hand side is negative for the scaling parameter λ small enough. Moreover, since the support of μ is compact, one can choose a sequence $\{\lambda_n\}$ such that $\lambda_n \rightarrow 0$ as $n \rightarrow \infty$ and the **supports of ψ_{0,λ_n} are mutually disjoint** which means that the discrete spectrum of H_r is infinite, accumulating at the threshold $(2a_0)^{-2}$. \square

Fermat meets Archimedes



As an example, consider an interpolation between Fermat and Archimedean spirals, in the simplest case described parametrically as

$$r(\theta) = a\sqrt{\theta\left(\theta + \frac{b^2}{a^2}\right)}, \quad a, b > 0,$$

with the asymptotic behavior

$$r(\theta) = b\sqrt{\theta} + \frac{a^2}{2b}\theta^{3/2} + \mathcal{O}(\theta^{5/2}),$$

$$r(\theta) = a\theta + \frac{b^2}{2a} + \mathcal{O}(\theta^{-1})$$

for $\theta \rightarrow 0+$ and $\theta \rightarrow \infty$, respectively.

Fermat meets Archimedes



As an example, consider an interpolation between Fermat and Archimedean spirals, in the simplest case described parametrically as

$$r(\theta) = a\sqrt{\theta\left(\theta + \frac{b^2}{a^2}\right)}, \quad a, b > 0,$$

with the asymptotic behavior

$$r(\theta) = b\sqrt{\theta} + \frac{a^2}{2b}\theta^{3/2} + \mathcal{O}(\theta^{5/2}),$$

$$r(\theta) = a\theta + \frac{b^2}{2a} + \mathcal{O}(\theta^{-1})$$

for $\theta \rightarrow 0+$ and $\theta \rightarrow \infty$, respectively.

The Fermat spiral is conventionally considered as a *two-arm one* dividing the plane into a pair of mutually homothetic regions, hence we interpolate with the two-arm Archimedean spiral; the essential spectrum is $[a^{-2}, \infty)$.

Fermat meets Archimedes, continued



As for the discrete spectrum, taking the expansion of $r(\theta)$ two terms further, we get $b_0 = \frac{b^2}{2a}$ and

$$\rho(\theta) = \frac{b^4}{8a^3\theta} - \frac{3b^6}{16a^5\theta^2} + \mathcal{O}(\theta^{-3}).$$

Fermat meets Archimedes, continued



As for the discrete spectrum, taking the expansion of $r(\theta)$ two terms further, we get $b_0 = \frac{b^2}{2a}$ and

$$\rho(\theta) = \frac{b^4}{8a^3\theta} - \frac{3b^6}{16a^5\theta^2} + \mathcal{O}(\theta^{-3}).$$

This means that the assumptions of the last proposition hold with $c = \frac{b^4}{8a^3} > 0$ and $\gamma = 2$, and the operator H_r has an *infinite discrete spectrum* in $(0, a^{-2})$ accumulating at the threshold.

Fermat meets Archimedes, continued



As for the discrete spectrum, taking the expansion of $r(\theta)$ two terms further, we get $b_0 = \frac{b^2}{2a}$ and

$$\rho(\theta) = \frac{b^4}{8a^3\theta} - \frac{3b^6}{16a^5\theta^2} + \mathcal{O}(\theta^{-3}).$$

This means that the assumptions of the last proposition hold with $c = \frac{b^4}{8a^3} > 0$ and $\gamma = 2$, and the operator H_r has an *infinite discrete spectrum* in $(0, a^{-2})$ accumulating at the threshold.

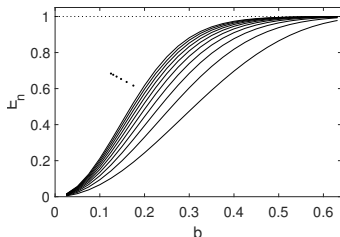
One can also specify the accumulation rate: the one-dimensional effective potential is in this case $\frac{\pi b^4}{16a^5} s^{-1} + \mathcal{O}(s^{-3/2})$, with the leading term of Coulomb type, which shows that the number of eigenvalues *below* $a^{-2} - E$ behaves as

$$\mathcal{N}_{a^{-2}-E}(H_r) = \frac{\pi b^4}{32a^5} \frac{1}{\sqrt{E}} + o(E^{-1/2}) \quad \text{if } E \rightarrow 0+$$

Eigenvalues



Let us plot the lowest eigenvalues of such a region as functions of b :

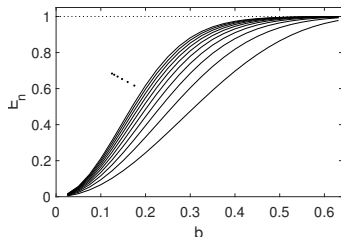


As expected the ground state is close to the continuum threshold for (sufficiently) large values of b and the *whole discrete spectrum disappears in the limit $b \rightarrow \infty$*

Eigenvalues



Let us plot the lowest eigenvalues of such a region as functions of b :

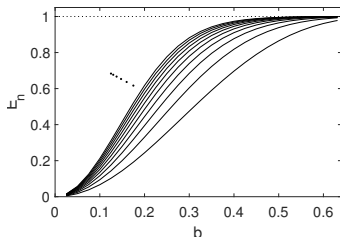


As expected the ground state is close to the continuum threshold for (sufficiently) large values of b and the *whole discrete spectrum disappears in the limit $b \rightarrow \infty$* , while for small b the region has *a large bulge* in the center and the spectral bottom drops to appropriately low values.

Eigenvalues



Let us plot the lowest eigenvalues of such a region as functions of b :



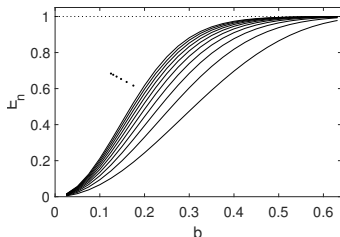
As expected the ground state is close to the continuum threshold for (sufficiently) large values of b and the *whole discrete spectrum disappears in the limit $b \rightarrow \infty$* , while for small b the region has *a large bulge* in the center and the spectral bottom drops to appropriately low values.

Remark: Experimentalists often label their spirals as Archimedean, but in fact *they are not*, being produced by coiling fibers of a *fixed cross section*, hence their transverse width is *constant* with respect to θ , in contrast to the true Archimedean spiral

Eigenvalues



Let us plot the lowest eigenvalues of such a region as functions of b :



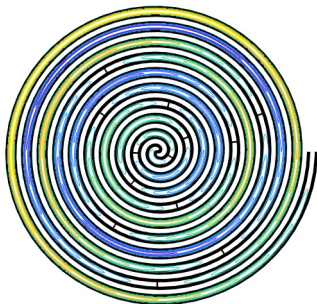
As expected the ground state is close to the continuum threshold for (sufficiently) large values of b and the *whole discrete spectrum disappears in the limit $b \rightarrow \infty$* , while for small b the region has *a large bulge* in the center and the spectral bottom drops to appropriately low values.

Remark: Experimentalists often label their spirals as Archimedean, but in fact *they are not*, being produced by coiling fibers of a *fixed cross section*, hence their transverse width is *constant* with respect to θ , in contrast to the true Archimedean spiral. Such waveguides behave asymptotically rather as the current interpolation with $\frac{b}{a} = (2\pi)^{-1/4} \approx 0.632$.

An eigenfunction example



Here is the eigenfunction with $E_{14} = 0.999952$ referring to $b = (2\pi)^{-1/4}$.



The difference from the two-arm Archimedean region is *hardly perceptible by a naked eye*, however, the discrete spectrum is now not only non-void but it is rich with the eigenfunctions the tails of which have a distinctively *quasi-one-dimensional character*.

What to bring home from Lecture II



- If a particle is confined to a hard-wall tube, a nontrivial geometry of the confinement gives rise to an *effective interaction*, attractive in case of bends.

What to bring home from Lecture II



- If a particle is confined to a hard-wall tube, a nontrivial geometry of the confinement gives rise to an *effective interaction*, attractive in case of bends.
- This effect is robust. not restricted to bends, and of a *genuine quantum nature* having no classical counterpart

What to bring home from Lecture II



- If a particle is confined to a hard-wall tube, a nontrivial geometry of the confinement gives rise to an *effective interaction*, attractive in case of bends.
- This effect is robust. not restricted to bends, and of a *genuine quantum nature* having no classical counterpart
- If the particle motion is restricted to a layer of constant width, it is the *global geometry* of the confinement that plays a decisive role.

What to bring home from Lecture II



- If a particle is confined to a hard-wall tube, a nontrivial geometry of the confinement gives rise to an *effective interaction*, attractive in case of bends.
- This effect is robust. not restricted to bends, and of a *genuine quantum nature* having no classical counterpart
- If the particle motion is restricted to a layer of constant width, it is the *global geometry* of the confinement that plays a decisive role.
- The existence of bound states in spiral waveguides depends on the asymptotic behavior of their width; the problem is subtle in the *asymptotically Archimedean* case.

What to bring home from Lecture II



- If a particle is confined to a hard-wall tube, a nontrivial geometry of the confinement gives rise to an *effective interaction*, attractive in case of bends.
- This effect is robust. not restricted to bends, and of a *genuine quantum nature* having no classical counterpart
- If the particle motion is restricted to a layer of constant width, it is the *global geometry* of the confinement that plays a decisive role.
- The existence of bound states in spiral waveguides depends on the asymptotic behavior of their width; the problem is subtle in the *asymptotically Archimedean* case.
- In contrast to mathematics, '*physicist's Archimedean waveguides*' have numerous weakly bound states.